Quantifying Surface Subsidence along US Highway 50, Reno County, KS using Terrestrial LiDAR

Submitted to the Department of Geology
In partial fulfillment of the requirements for the
Degree of Master of Science

Andrew J. Herrs
B.S., Kansas State University, 2008

Advisory Committee:

_____
Michael H. Taylor (Chair)

_____
W. Lynn Watney

_____
J. Douglas Walker

Date of Thesis Defense: April 21, 2010

[Acceptance Page for Thesis]

The Thesis Committee for Andrew J. Herrs certifies that this is the approved version of the following thesis:

Quantifying Surface Subsidence along US Highway 50, Reno County, KS using Terrestrial LiDAR

Advisory Committee:

_____
Michael H. Taylor (Chair)

_____
W. Lynn Watney

_____
J. Douglas Walker

Date Approved: April 21, 2010

ABSTRACT

US-50 in Reno County, KS east of Hutchinson has undergone active deformation from ground subsidence. Subsurface karsting from salt dissolution is the main cause for this phenomenon. Two prominent sinkhole features occur in close proximity to one another and to the regionally mapped dissolution front of the Hutchinson Salt Member. Brandy Lake, which is a lake forming sinkhole, has undergone active subsidence along its western margin whereas the sinkhole at the Victory Road/US-50 intersection has had subsidence occur within the last 12 years. Using a Terrestrial Laser Scanning (TLS) approach, this study analyzes the geometry, magnitude and temporal nature of the active subsidence over these two sinkholes. Results show that the Brandy Lake sinkhole has an asymmetric subsidence geometry along the western margin of the lake with a deformed road area of 358 m and a magnitude of subsidence of 1.15 m. The Victory Road sinkhole is characterized by a symmetric bowl-shaped depression that is 125 m wide from west to east and 117 m wide from north to south with a magnitude of subsidence of 1.20 m. Both of the sinkholes exhibit no active change over the course of the study indicating that subsidence has temporarily ceased. These observations agree with the fact that subsidence is transient on the local scale but regionally controlled by the main dissolution front and subsurface structural lineaments.

DEDICATION

I would like to dedicate my work on this project to my family and friends and to thank them for their support.

To the friends that I've made at both K-State and KU, it's been great to share many laughs and of course my interest for geology.

To my friends since middle school, Derrick, Kevin and Tom, you three have been my best friends who I can always trust.

To my family in the Philippines, I'm fortunate to have such great Kuyas, Ates, Titas and Titos to show me what it means to be Pilipino and how to represent our culture the best way possible. *Mahal na mahal kita!*

To Mau, my significant other. You inspire me to be someone more. Someone more accountable, more trustworthy, and more selfless. I'm glad that I can think about the future and know that we'll be happy, together.

Finally to Dad, Mom and my sister Diana, thank you so much for believing in me. Dad, you've taught me so much about how the world works and to think for myself. Mom, you've taught me that the I have to work hard and have a good heart to earn respect and success. And Diana, even though you may not realize it, you're always smiling and I always try to look at the bright side of life because of you. To you three, I owe everything that I am to you. My accomplishments are yours and I love you with all my heart and soul.

ACKNOWLEDGEMENTS

I would first like to thank my advisor, Mike Taylor, for providing direct oversight and guidance to this project and my other endeavors during my time at KU. Thanks to my other committee members, Doug Walker for help with LiDAR operation and procedures, and Lynn Watney for explaining the past research associated with this project and the implications for this work. Rick Miller also helped to explain the implications for using LiDAR to study sinkholes.

From the Riegl USA, I would like to thank Jennifer Triana and Tan Nguyen for LiDAR training and software assistance. Additional assistance with LiDAR operation and maintenance was aided by Brett Bennett of the Kansas Geological Survey. Initial scouting of the study area was done with the help of Bob Henthorne from KDOT. LiDAR acquisition at each project site was accomplished with the help of Nick Laskares, Willy Rittase, Ken Stalder, Mike Taylor, Lynn Watney, the Hutchinson KDOT maintenance crew, and KDOT's Salina Regional Geology Department. Kwan Yee Cheng and Richard Styron also helped with plotting data in MATLAB. ArcMap techniques were demonstrated by Prabin Shilpakar from the University of Texas-Dallas.

Funding for this project was provided by a grant from KU's Transportation Research Institute, NSF, and INTERFACE, as well as a student research grant from the Geological Society of America.

TABLE OF CONTENTS

FIGURE LIST

INTRODUCTION

METHODS

CHAPTER 1

Introduction

Objective

Past research has employed different methods for studying subsidence features and how they relate to salt dissolution. Subsurface mapping techniques have been accomplished through well log correlation (Watney, 1980; Watney & Paul, 1980; Watney et al., 2003) and seismic reflection techniques (Anderson et al., 1998; Miller & Xia, 2002; Miller, 2009; Steeples et al., 1986). Mapping sinkhole features at the surface has also been done through Airborne Laser Swath Mapping (ALSM), and Interferometric Synthetic Aperture Radar (InSAR) techniques (Abelson et al., 2003; Baer et al., 2002; Seale et al., 2008). Furthermore, temporal studies have been conducted to analyze the evolution of sinkhole development (Soriano & Simon, 2002) and to attempt to develop hazard assessments for certain areas (Galve et al., 2009; Gutierrez et al., 2008).

In south central Kansas, several subsidence features have formed from two different causes: rapid dissolution of salt from poorly abandoned wells, and gradual dissolution by infiltration of under saturated ground water. The former case has been studied thoroughly through the techniques listed above, but the natural occurrence of gradual karsting and the resulting surface subsidence is not as well understood. Also, the complex nature of the area, with an active salt dissolution front and a network of subsurface faults contributes to active sinkhole development.

This study utilizes the innovative technology of Terrestrial LiDAR (Light Detection And Ranging) and other approaches to develop a spatial and temporal characterization of two different active sinkholes in Reno County, Kansas. There are

multiple advantages in using terrestrial LiDAR. First, the LiDAR scanner acquires data of the terrain with high precision where the uncertainty in the points is only a few centimeters. Therefore, the resulting point cloud is an accurate representation of the true object or terrain. The scanner also is able to gather up to hundreds of points per square meter which yields a high density of points for an area. The rate at which the scanner collects these points is up to 11,000 points per second which allows for each project site to be scanned within one day. Lastly, with GPS equipment, the LiDAR datasets are able to be georeferenced and compared with data from a time series of scans gathered over the same project site. Therefore, the scanning data are able to image the spatial characteristics of the sinkholes accurately. By doing this, the observations in this study can be compared with past work that analyzes naturally occurring sinkholes from their subsurface characteristics. Therefore, this study can provide insight to the quantitative characteristics of sinkholes in south central Kansas.

The process of salt dissolution and its effects are described in the following sections. Specific mechanisms for salt dissolution and surface subsidence are also explained with an emphasis on how salt dissolution is occurring in south central Kansas. In addition, the approach of this study is to use the innovative remote sensing technique of LiDAR imaging to understand sinkhole characteristics. Since this is a relatively new approach, LiDAR concepts and methods are described. Finally, the results and interpretations from this study are presented to strengthen our understanding of natural salt dissolution and surface subsidence in south central Kansas.

Salt Dissolution

Subsurface karsting and the resulting surface subsidence features are problematic for various reasons. Karsting can compromise the integrity of infrastructure such as roadways, buildings and utility lines (Guerrero et al., 2004; Gutierrez et al., 2008; Waltham, 2008). Subsidence sinkholes can render these elements unsafe as they become costly and time consuming to repair (Croxton, 2002). Examples from Soriano & Simon (1995 & 2002) illustrate the widespread residential damage due to active ground subsidence. Walters (1978) profiles one particular sinkhole in Hutchinson, KS that left a railroad track suspended in midair as a result of catastrophic sinkhole development. Understanding this phenomenon is essential for better understanding the salt dissolution process and to avoid expensive maintenance and safety hazards.

Dissolution Process

Dissolving evaporites and carbonates create karst features that shape the landscape. In terms of karst formation, the main difference between carbonates and evaporites is the dissolution rate. Evaporites (halite, gypsum, and anhydrite etc.) and carbonates (limestone and dolomite) dissolve into aqueous solution when in contact with undersaturated water. However, dissolution in carbonates is also due to the presence of weak acids in undersaturated water. Limestones and dolomites have a solubility of 0.5 g/l (depending on the pH of the fluid), while gypsum and halite have solubilities of 2.4 and 360 g/l respectively (Gutierrez et al., 2008). The fact that halite has a solubility 2 orders of magnitude higher than gypsum is the main reason that halite does not crop out

in humid or temperate climates. Therefore, the formation of karst features by evaporite dissolution is quick and unpredictable.

Evaporite rock layers cover a large area in the subsurface of the North America and elsewhere in the world. The mechanisms in which these evaporites dissolve are important to understand how dissolution is initiated and sustained. In most areas, there are two main dissolution mechanisms that are best described by Anderson & Knapp (1993). The first is centripital flow which involves leaching an evaporite layer with undersaturated ground water via proximal aquifers. Permeability is higher in these aquifers and therefore provides a conduit for ground water flow. The natural movement of the water provides a mechanism to continuously leach the evaporites from their solid state. The second mechanism is evaporite dissolution from contact with undersaturated water that flows through subsurface faults and fractures. The rate of fluid movement through open fractures can be significantly higher than through the pore space of consolidated strata. Therefore the dissolution rate can also increase.

Anthropogenic activities also contribute to karst development in some areas (Anderson et al., 1998; Walters, 1978; Watney et al, 2003). In south-central Kansas, throughout most of the 1900's many oil wells were drilled. These wells tapped into the Hutchinson Salt Member which was coined as the "lost circulation zone" when drillers would pass through it due to its high solubility, low strength and contact with the drilling fluid. Eventually some of these wells lost their productivity and went offline. Improper abandonment procedures in the form of weak casings or insufficient sealing around the well bore provided undersaturated brine to infiltrate the salt layer (Walters, 1978). This

free access to undersaturated water rapidly leaches away salt in the subsurface thereby creating large void spaces.

Effects of Salt Dissolution

The dissolution mechanisms described in the previous section give way to instabilities in the overlying strata. Subsequently, if the overburden stress becomes too great, the overlying rocks settle or collapse into the underlying void space. Depending on the nature of the void and the composition of the overlying strata, the subsidence can be gradual (cm's/yr) or catastrophic (m's/day). Examples of both end member scenarios are seen in Croxton (2002) and Walters (1978) (Figure 1). These two end member cases are similarly addressed as suffusion/sagging sinkholes or collapse sinkholes (Gutierrez et al., 2008). Collapse sinkholes often occur as real void space is created and then filled by collapsing the above rock layers into the void (Figure 2). This has the possibility of being a sudden, catastrophic event. Sagging or suffusion sinkholes gradually subside because of a slower dissolution rate or because of unconsolidated overlying sediments that deform more gradually (Figure 3). The latter scenario often occurs in evaporites that have layers of overlying alluvium.

Subsidence that occurs from large scale subsurface karsting influences the depositional patterns of fluvial channels in some cases by changing the local base level. The topographic lowering of the surface due to subsidence in south-central Kansas has formed sediment accommodation zones. The increased influx of undersaturated water from these fluvial sources can cause increased dissolution of the salt as well. In effect, a

positive feedback mechanism is created whereby the dissolution process is enhanced (Anderson et al., 1994; Watney et al., 2003).

Another area where fluvial systems are influenced by evaporite karsting is the Ebro Basin in Spain. Here, evaporites mantled by alluvial deposits occur at or near the surface. However, where dissolution has occurred, a thickening of the alluvial sediments is observed (Gutierrez et al., 2008). This thickening is again due to gravitational lowering of the surface and deposition in these subsidence areas. In other cases, local farmers have back-filled the subsidence features, therefore masking their surface expression and making them harder to detect (Soriano & Simon, 2002).

In the tectonically active area of the Dead Sea in Israel, near-surface active structures exert a strong control on karst development and sinkhole distribution. Normal faulting along the Dead Sea margins provides a path for shallow evaporites to be leached (Abelson et al., 2003; Closson, 2005; Closson et al., 2005). Because these structures and evaporites are near the surface, the resulting sinkholes are highly concentrated along the faults. Furthermore, due to withdrawal of the Dead Sea water throughout the past century, rapid karst features have developed, giving way to the rapid formation of sinkholes. The sinkholes are so common, that their linearity gives an accurate first order indicator to the location of the rift bounding normal faults. This direct correlation to sinkhole distribution is important for understanding other areas where structural elements play a role in evaporite leaching and the occurrence of subsidence features.

In many parts of the world, evaporite dissolution is a complex phenomena that is driven by tectonic perturbations, fluvial systems, and undersaturated water movement. By analyzing these examples, forming explanations for dissolution of the Hutchinson Salt

Member are possible. Each of the mechanisms for salt dissolution are important in analyzing any area of subsurface evaporite karsting.

Geologic Background of Reno County, Kansas

The Hutchinson Salt Member is a massive evaporite layer in south-central Kansas that is locally up to 250 m thick (Figure 4). The evaporite has been a major source of rock salt mining for a large part of the 1900's-present (Walters, 1978). It is part of the larger Wellington Formation which mainly consists of gray shales interbedded with argillaceous limestone and dolomite intervals in addition to the Hutchinson Salt. Above the Wellington Formation lies the Ninnescah Shale. The Ninnescah Shale is made up of red and gray shales with interbedded argillaceous limestone and dolomite. This entire stratigraphic sequence is within the Lower Permian Sumner Group which has an average thickness of 300m. Underlying the Sumner Group is the Lower Permian Chase Group (Merriam, 1963; Zeller, 1968).

The salt was deposited as a cyclic shelf deposit where it was able to precipitate out in a semi-arid climate as the sea level regressed toward the southwest. This smaller epicontinental sea previously encroached into what is now the central US. Subsequent transgression of sea level accounts for the deposition of the overlying shales in the Sumner Group. The Hutchinson Salt Member occupies 37,000 km^2 in the subsurface. Because of subtle tectonic influences since the Permian, a gradual westward dip in the Permian units is observed (Figure 5). Specifically, early Tertiary orogenesis in the form of flexural loading around the western US is the main cause for the west dipping strata (Watney, 1980; Watney & Paul 1980).

The Permian strata in south-central Kansas are overlain by the Quaternary Equus Beds which is a freshwater aquifer. These beds are up to 30 m thick in Reno County and were deposited during different episodes of alluvial deposition during the Quaternary. The Quaternary deposition of these alluvial beds was a result of an increased topographic gradient east to west which directed stream paths down from the Rockies and into the High Plains, and south below the Flint Hills of Kansas (Lane & Miller, 1965).

Along its western, southern, and northern margins, the salt depositionally pinches out and interfingers with the overlying shale units. However, along the eastern margin, the salt exhibits an abrupt isopach discontinuity (Figure 4). This is the natural dissolution front that has been studied and mapped over the past 4 decades (Anderson et al., 1998; Walters, 1978; Watney & Paul, 1980; Watney et al., 2003). This is generally the only area where natural dissolution of the salt occurs. Further to the west of this dissolution front, the overlying shale units act as aquitards to seal the Hutchinson Salt from any encroaching ground water. Therefore, many of the dissolution features further to the west of the main dissolution front are dominantly anthropogenic in origin. The westward migrating dissolution front was able to propagate because of the westward dip of the Permian layers. In other words, the eastern margin was more accessible to undersaturated ground water and thus this is where preferential leaching occurs.

Accessibility to ground water is not the only reason that dissolution was initiated on the eastern margin. Inherited basement topography exerts strong controls on where the Hutchinson Salt is leached. In particular, magnetic and gravity data from Kruger (1995) shows a significant basement high that trends NNE across eastern Reno County and into McPherson County (Figure 6). This high, termed the Voshell Ridge (Merriam,

1963; Watney et al., 2003) has folded the Permian sediments that overly it. Structural features have been mapped along the western slope of the Voshell Ridge (Xia et al., 1995; Nissen & Watney, 2004). These include tensional fractures formed from increased depositional loading, similar to what was described by Anderson & Knapp (1993). These features were likely reactivated due to farfield stresses. The current extent of the dissolution front is along one of these fractures which is likely enhancing the dissolution process. Several other faults are interpreted by Watney et al. (2003) and Nissen & Watney, (2004) to run parallel to the Arkansas River to the southwest of Hutchinson (Figure 6). The main structural feature, known as the Arkansas River Lineament, has exhibited a strong control on the alignment of the Arkansas River Valley in northeast Reno County (Nissen & Watney, 2004).

Study Area

Brandy Lake

The area of Brandy Lake in Reno County, Kansas is east of Hutchinson by a few kilometers along US-50 (Figure 7). Submerged trees in the immediate vicinity and the nature of the shorelines at Brandy Lake suggest that it is a lake forming sinkhole. The active deformation along its western margin is the most useful to monitor deformation because US-50, which runs east-west, was built directly through the middle of the lake (Figure 8). Therefore, the surface of the highway itself has provided an accurate strain marker with which to analyze surface subsidence (Figure 9).

Victory Road

Victory Road is a north-south secondary county road that crosses US-50 three kilometers east of Brandy Lake (Figure 10) and is the location of an active sinkhole. US-50 again acts as a strain marker for the deformation that has taken place (Figure 11). Also, the Victory Road sinkhole has had recent repavement projects to compensate for the subsidence (Figure 10). The Kansas Department of Transportation estimates that up to 1.0 m of additional asphalt was laid on the surface of US-50 to mitigate the effects of surface subsidence.

Both of these sinkhole features provide an opportunity to study the evolution of sinkhole development in an active evaporite karst setting. Each of these features is located where the active dissolution front of the Hutchinson Salt Member resides. Additionally, important subsurface structural features such as the Voshell Ridge and the associated north-northeast and west-northwest striking faults and fractures that occur in the area.

Light Detection and Ranging (LiDAR)

In this study, Ground-Based LiDAR was used to conduct a geologic investigation to understand the spatial and temporal evolution of evaporite karsting. To understand how this technique is useful for Earth science studies, a description of LiDAR is given below.

LiDAR is an innovative remote sensing technique, somewhat similar to RADAR (Radio Detection And Ranging). LiDAR uses electromagnetic (EM) energy to measure the distance between the LiDAR instrument that emits an EM pulse, and the object that

that pulse reflects off of. However, the difference between RADAR and LiDAR is significant. While RADAR utilizes EM energy in the long, radio wavelength part of the EM spectrum, LiDAR utilizes energy in the Near Infrared wavelength (800-2500 nm) range (Figure 12). Because of this contrast in wavelength of the emitted energy, LiDAR techniques are able to image objects at a much higher resolution than RADAR. For this study, the LiDAR resolution was anywhere from 10 points/m^2 at distances of 500 m to over 500 points/m^2 within 2 m of the sensor.

Understanding the way real Earth objects are imaged with LiDAR is important. As previously stated, a LiDAR instrument constructs high precision 3D representations of objects. By emitting thousands or millions of EM pulses, the LiDAR collects a 3D point cloud where each point represents an X,Y,Z coordinate (Figure 13). In addition to coordinate values, LiDAR can also reveal surface characteristics of an object based on the reflected intensity of the returned LiDAR pulse. For example, mirrors or reflective surfaces such as street signs will return a higher intensity value than a tree or building. Certain LiDAR instruments also store echo data from an object. Each LiDAR point can store the quality of its return in the form of its echo characteristic. In general, what are termed "last return" points are usually from broad, solid objects that the LiDAR pulse cannot physically penetrate. "First return" and "middle return" points usually reflect off of vegetation or smaller objects that the LiDAR pulse can penetrate.

LiDAR acquisition fits into three main categories: Terrestrial Laser Scanning, Mobile scanning, and Airborne Laser Swath Mapping (ALSM). Terrestrial Laser Scanning (TLS), or Ground-based LiDAR, is accomplished by placing a LiDAR scanner at a fixed point, often on top of a stationary tripod, and then scanning an area or object of

interest. Mobile scanning involves mounting a LiDAR scanning instrument on a vehicle and gathering data while the vehicle is traversing the area of interest. ALSM places a LiDAR scanner on the bottom of an aircraft. Data is then gathered in several kilometer long strips across a landscape. Each LiDAR acquisition technique serves its own purpose. Terrestrial LiDAR scanning is useful for producing cm-scale, high resolution data over smaller areas while Mobile scanning and ALSM are able to cover larger study areas and produce sub-meter scale, lower resolution data. For long term projects where LiDAR is needed over the course of several months or years, Terrestrial Laser Scanning is also more cost effective. The bulk of the cost for TLS data is for the purchase of the scanner itself. Therefore, using a terrestrial laser scanner is more financially feasible approach as well.

For geologic purposes, particularly smaller localized features, TLS techniques are useful for attaining surface data of rock outcrops (Bellian et al., 2005), fault scarps, and in areas of dense vegetation (Nagihara, 2006; Tarolli et al., 2009). This method is also more accurate to georeference since it stays at a fixed point while scanning. Therefore it does not need to undergo any flightline or orientation corrections as is often the case with ALSM data. Sometimes flightline edges of ALSM data can distort the LiDAR point clouds to the point where there is over 0.3 m of mismatch (Shrestha et al. 1999).

Figure 1:
(*A*) Evidence of structural damage from subsurface evaporite karsting. Gradual subsidence results in subtle flexure in the road surface over the span of the sinkhole as observed by Croxton (2002) A westward looking photo along I-70 in Russell County, KS across the Crawford sinkhole. (*B*) Catastrophic collapse features studied by Walters (1978) form over short time spans and are capable of significant damage to man-made structures. In 1974, a catastrophic sinkhole formed near the Cargill salt mine in McPherson County, KS. This sinkhole formed from underground salt mining which created a large void space.

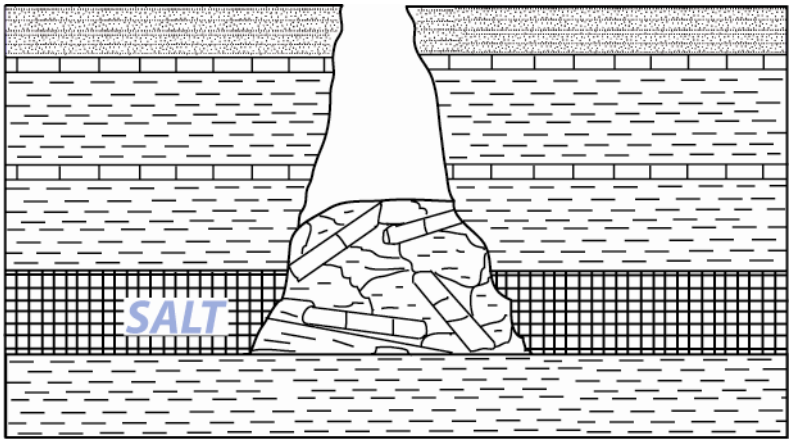

Figure 2:
A collapse sinkhole described by Gutierrez et al (2008) features steep sided walls where failure surfaces are created. The surface expression of these sinkholes is noticeable and unstable. Rapid salt dissolution can cause void spaces in the subsurface, similar to the sinkhole in Figure 1B.

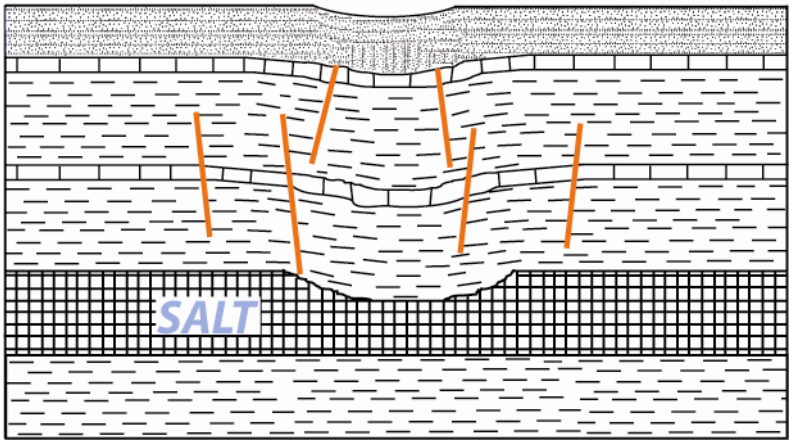

Figure 3:
Gutierrez et al. (2008) categorizes sagging sinkholes by gradual subsidence of rock layers by steady dissolution of an evaporite layer at depth. Small scale faults (orange lines) and fractures are able to develop in the strata overlying the salt causing the surface to sag and fold in a concave up geometry.

37°0'0"N
38°0'0"N
39°0'0"N
40°0'0"N
95°0'0"W
97°30'0"W
100°0'0"W
Topeka
Lawrence
A
B
0
30
60
90
milligals
45
-25
Km
0
30
60
120
N

Figure 4 (previous page):
Isopach map showing the extent of the Hutchinson Salt Member in south central Kansas as mapped by Watney et al. (2003) with Residual Bouguer gravity data from Xia et al. (1995). The salt reaches a maximum thickness of over 90 m southwest of the study area. The northern, western, and southern margins of the salt depositionally pinch out. The eastern margin of the salt features a westward advancing dissolution front as indicated by the steep isopach margin. Part of the main dissolution front occurs in eastern Reno County, KS (shaded white) and east of Hutchinson (white circle marker). Cross section A-B is shown in Figure 5.

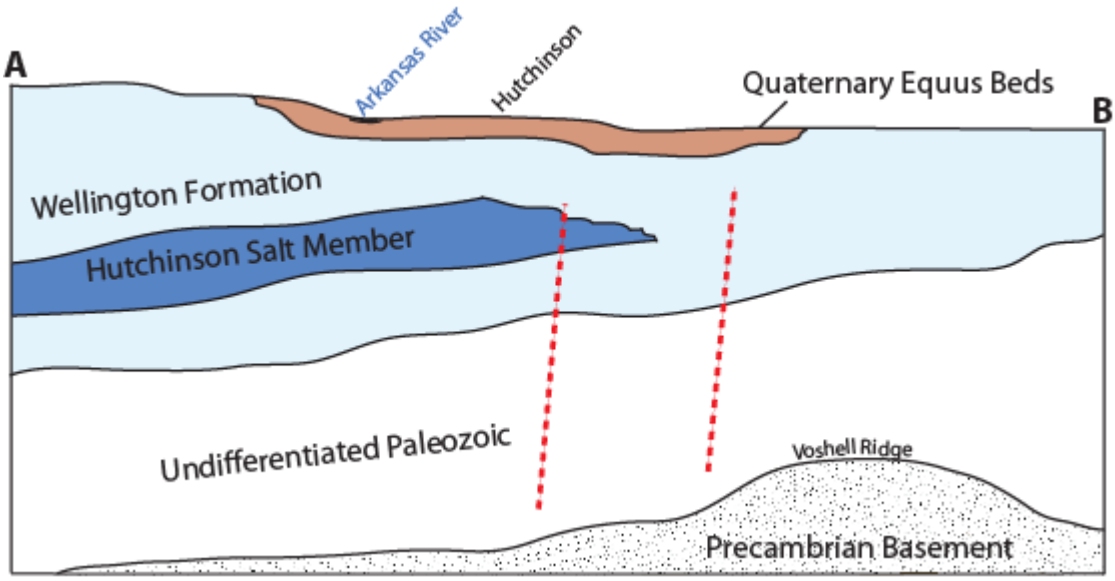

Figure 5:
Cross section line A-B from Figure 4. The Hutchinson Salt Member and Wellington Formation dip westward at ~6 m/km (Watney et al, 2003). The Wellington Formation, which is part of the Sumner Group, overlies the Chase Group. In Reno County, the Quaternary Equus Beds are an incised valley fill system that downcut through the Permian strata. Subsurface fracturing as interpreted by Xia et al. (1995) and mapped as dashed red lines. Stratigraphy is displayed according to Walters (1978).

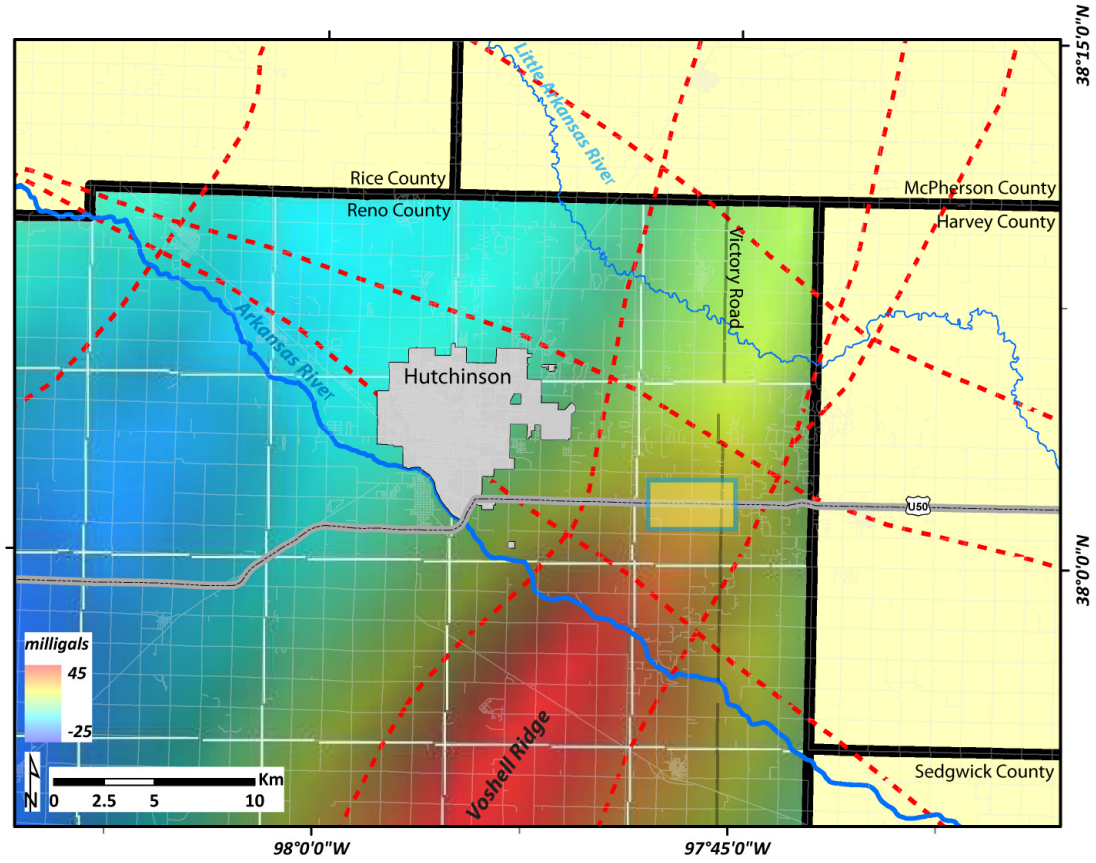

Figure 6:
The main active dissolution front runs through eastern Reno County. The Voshell Ridge , shown as a red gravity anomaly, is a structurally high basement feature that trends north-northeast as mapped by Xia et al. (1995) and Cole (1976). Other structural fractures, shown as red dashed lines, are oriented north-northeast and west-northwest which influence the path of the Arkansas River and other dissolution features observed in Reno County. US-50 and Victory Road traverse two sinkholes which are the focus of this study. The yellow fill/blue outlined inset polygon highlights the area displayed in Figure 7. Hutchinson's city limits are displayed as the gray region immediately north of US-50.

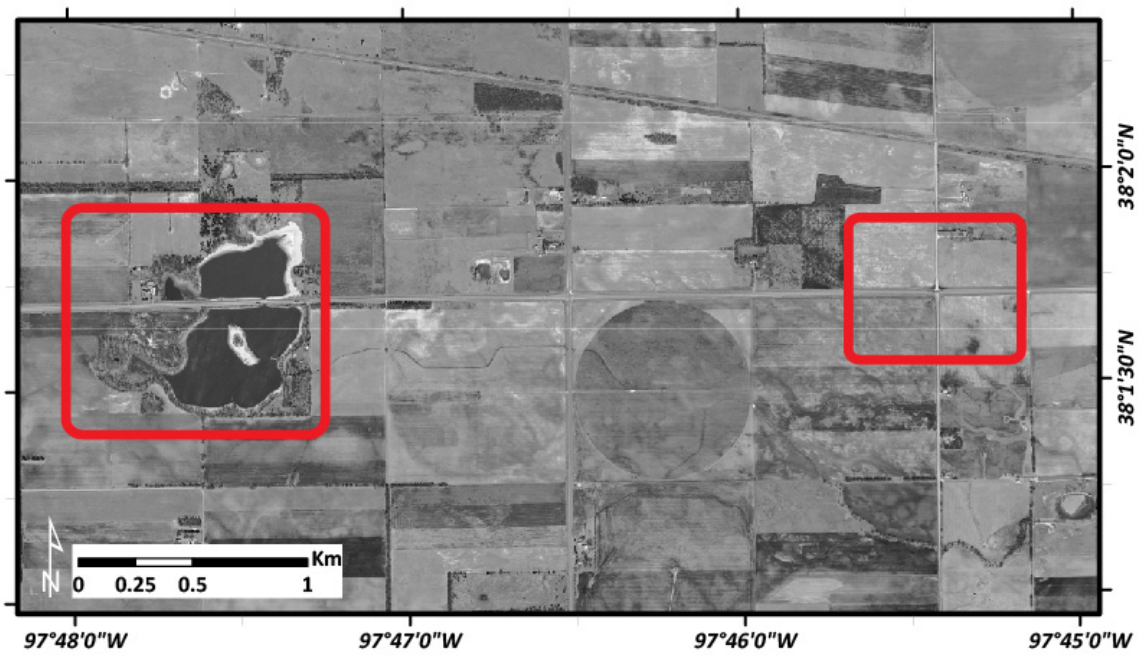

Figure 7:
Aerial photo of the study area highlighted in Figure 6. The Brandy Lake sinkhole is on the left, the larger red inset is shown in Figure 8. The Victory Road sinkhole is on the right, the smaller red inset is shown in Figure 10.

Figure 8:
Close up of Brandy Lake sinkhole where US-50 runs west-east over the middle of the lake. The red marker indicates where the photo in Figure 9 was taken as well as the look direction. See Figure 7 for location.

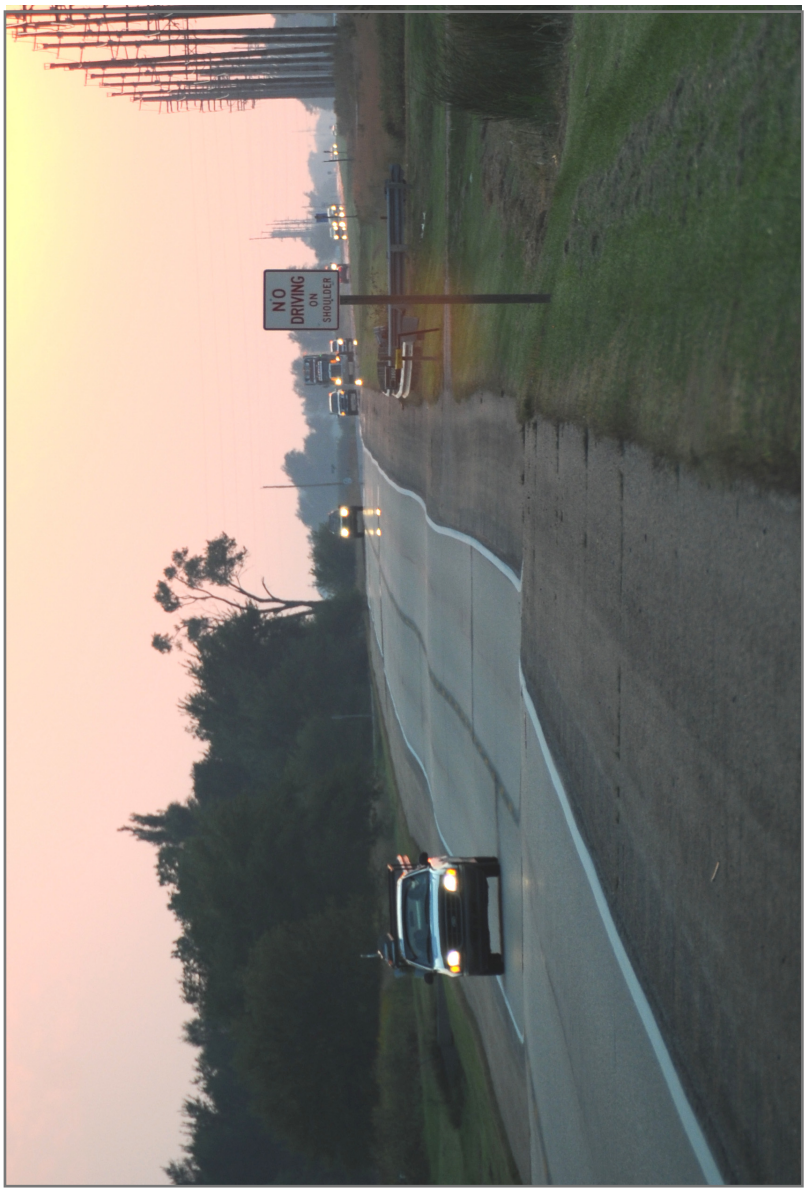

Figure 9:
A westward looking photo taken along US-50 at the western margin of Brandy Lake. Subsidence is observed as a subtle dip in the road surface just in front of the closest vehicle. This is the area of interest for gathering TLS data. See Figure 8 for location.

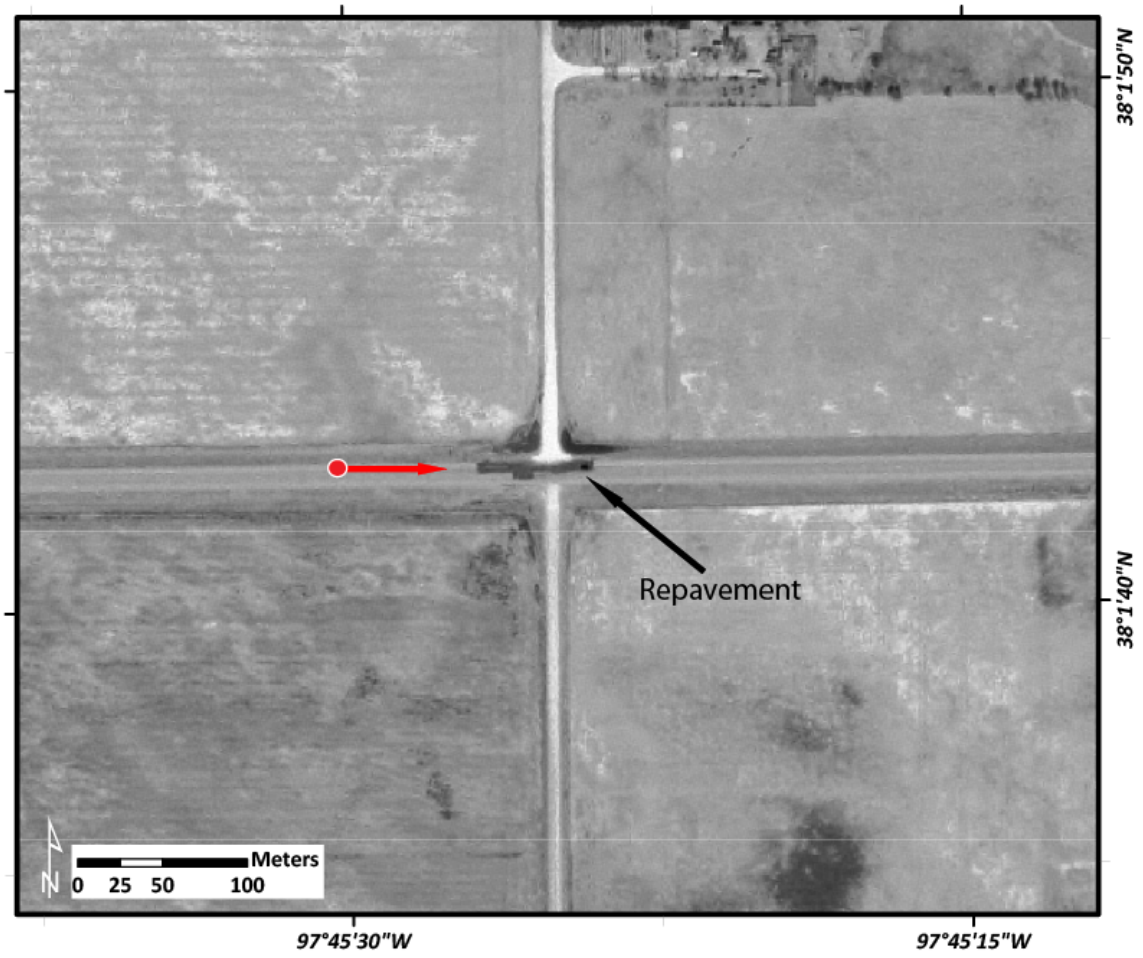

Figure 10:
Intersection of north-south running Victory Road and US-50. The black strip (indicated by the black arrow) on the north side of US-50 is a repaving project done by KDOT in response to surface subsidence of the road. The red marker indicates the look direction of the photo in Figure 11. See Figure 7 for location.

Figure 11:
An eastward looking photo taken along US-50 at the Victory Road intersection. The dip in the west-east fenceline is apparent as well as subtle subsidence at the intersection as indicated by the red arrow. A tiepoint reflector is photographed in the foreground as well. Tiepoint reflectors are a survey tool used to referenced LiDAR datasets. See Figure 10 for location.

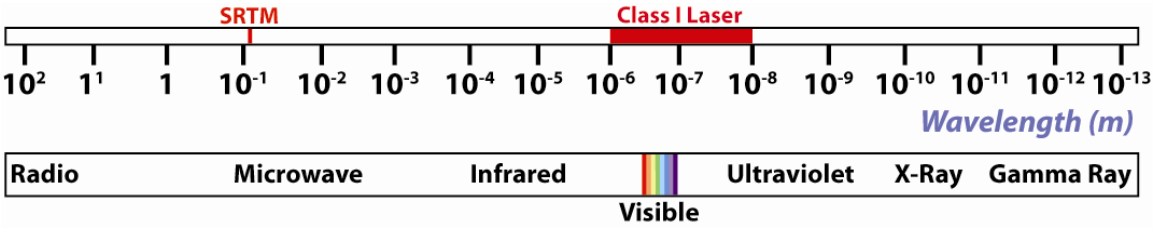

Figure 12:
The Electromagnetic Spectrum displays the range of wavelengths of different types of waves. For comparison, the Shuttle Radar Topography Mission (SRTM) used remote sensing wavelengths in the radio wave part of the spectrum. Class I lasers, such as the TLS scanner used in this study, use shorter wavelength energy to image smaller objects with higher resolution. Class I lasers use energy that is near the visible part of the EM spectrum. Both of these remote sensing techniques are displayed in red.

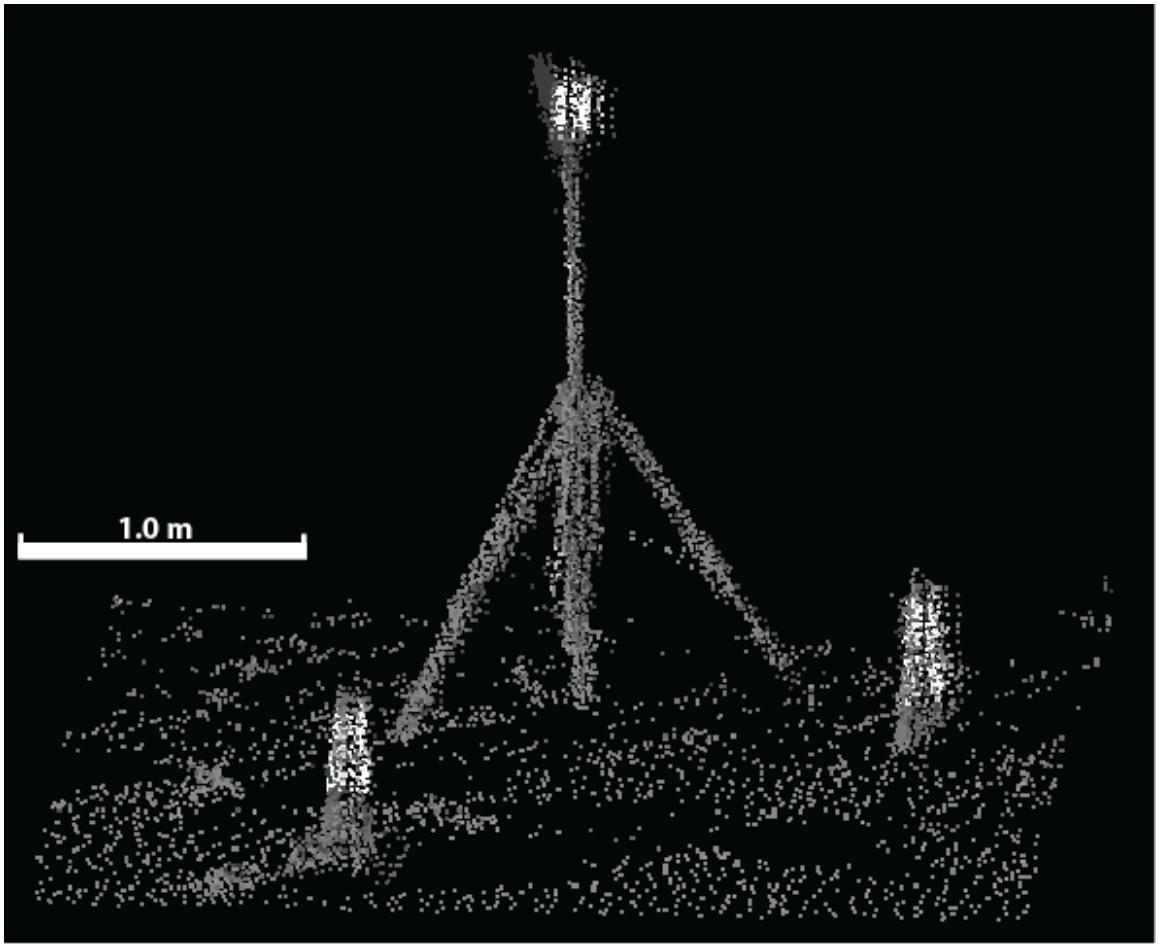

Figure 13:
LiDAR constructs a point cloud from a real world object or terrain. A tiepoint reflector is imaged here with a TLS scanner. This particular tiepoint reflector is a 10 cm cylinder reflector mounted to a tripod. The point cloud is colored by surface intensity. A tiepoint reflector is in Figure 11 for comparison. The two bright reflections to the left and right of the tiepoint reflector are traffic cones.

CHAPTER 2

Methods

Riegl LMS-Z620

A Riegl LMS-Z620 terrestrial LiDAR scanner was used in this study (Figure 14). It has a maximum range of 2.0 km in ideal conditions, a scanning rate of 11,000 points/second, and accuracy of about 1.0 cm. It is a Class I laser scanner that operates in the near infrared wavelengths (Figure 12). The range of vertical axis rotation for the scanner is 360° while the horizontal axis range of rotation is 80° (Figure 15). The scanner is completely portable and therefore operates from a DC converter that is powered by a 1000 w Honda gas-powered generator. It is operated with RiScan Pro software installed on a Panasonic Toughbook.

Pilot Study and Training Session

The Riegl LMS-Z620 terrestrial LiDAR scanner was acquired by the Kansas Geological Survey and the University of Kansas Department of Geology in July, 2008. To familiarize researchers and faculty with the scanner's capabilities, near-by sample areas were scanned. The first preliminary scan site was a road cut outcrop south of K-10 and east of Clinton Lake in Douglas County, KS. This scanning site was used to establish a scanning workflow for gathering field data. The second scan site was on the KU campus near the Kansas Geological Survey facilities in Lawrence, KS. The purpose of this second project site was to test the full range and capability of the scanner. With a better understanding of the utility of the scanner, the Hutchinson dissolution study was planned more effectively.

Identifying subsidence features

Although it is well known that regional subsidence has occurred and is well documented in the Reno County area (Miller, 2002; Anderson et al. 1994), preliminary field observations and past research were used to identify two subsidence features where this study could be conducted. The field observations were accomplished by discussions and scouting with the Kansas Department of Transportation's Chief Geologist Robert Henthorne. During September 2008, Henthorne noted that the two study sites at Brandy Lake and Victory Road had undergone resurfacing over the past decade. He was also able to approximately show where surface subsidence occurred at the two sites. At Victory Road, the active subsidence is concentrated northwest of the US-50 & Victory Road intersection. At Brandy Lake, subsidence is observed toward the western margin of the lake.

Reference points

Georeferencing of LiDAR data is an important step for time dependant analyses which this study is based on. If proper georeferencing procedures are conducted, any changes in the terrain can be seen in LiDAR data sets that were gathered up to a few months apart. Therefore, the placement of permanent monuments was completed for use as reference points (Figure 16). These permanent monuments were placed outside of the known deformation areas. Therefore, each iterative LiDAR survey over the next 18 months would have a stable ground point to be referenced to. The Victory Road site has three monuments, two outside and one inside the subsidence feature (Figure 17). Brandy Lake has seven, four at the corners of a bridge in the middle of the lake, two on either end

of the lake, and one in the active deformation zone (Figure 18). More monuments were placed at the Brandy Lake sinkhole because it is a considerably larger subsidence feature and also because the bridge that traverses Brandy Lake has accurate Stationing and Offset measurements. These Stationing and Offset measurements are points referenced to a UTM coordinate system that could be used for spatial referencing to serve the purposes of KDOT.

Subsequently, in September 2008, the marked points for the permanent monuments were drilled by KDOT's Salina Geology drilling crew. Each monument was drilled with a 4 in. auger bit 6 ft into the ground. 5/8 in. rebar was then placed in the center of each hole and grouted for stability. The end result had each monument even with the ground surface which is identifiable and easy to locate (Figure 16).

Initial Scanning Survey

The first scanning survey took place on October 30-31, 2008. Victory Road was the first site surveyed. Real Time Kinematic - Global Positioning System (RTK-GPS) points were the first data to be gathered and imported into the LiDAR software, RiScan Pro 1.4.3. This was accomplished by assembling the Trimble 5800 RTK-GPS equipment in the middle of the study area along Victory Road and south of US-50. The GPS point data were collected with Trimble's RTK roving GPS surveyor and TSC2 data collector that were attached to a range pole to increase the accuracy and placement above each of the monuments (Figure 19). Importing and georeferencing points gathered from the RTK-GPS data collector were successful for the Victory Road sinkhole. Horizontal and vertical errors of the GPS control points were 1.5-2.8 cm standard deviation respectively.

The LiDAR scanner was then set up at five different locations at the Victory Road/US-50 intersection (Figure 17). The purpose of setting up the scanner in several locations for a project site is to acquire complete data coverage of that site. If only one scan position were used, there would not be enough data to construct a ground surface model for the area because the scanner cannot collect point returns from behind telephone poles or other terrain features which block the scanner's view. Several tiepoints were set up in the project area to merge the LiDAR scans (Figure 19). At each scan position, a 15-25 minute finer-resolution scan was taken. The resolution for these fine scans was 0.020 - 0.025 milrad depending on the scan angle that was taken and to maximize field time. At this resolution, the resulting point densities would be ~50 points/m^2 for an area 100 m from the scanner. Scans of large angles up to 180° would be gathered with a lower resolution (0.100 milrad).

The Brandy Lake RTK-GPS points proved to be more difficult to georeference with the LiDAR data due to reasons that are addressed in the next section. The scanner was set up 6 times along the length of US-50 beginning at the western margin of the lake (Figure 18).

Additional Scanning Surveys

Subsequent scanning surveys were conducted as weather and time permitted throughout 2009 and 2010. There are 6 total surveys from October 2008, February/May/September/November 2009, and February 2010. The same amount and areas of data were gathered for Brandy Lake and Victory Road during each survey.

Data quality on each survey is influenced primarily by passing traffic along US-50 generating wind turbulence during the scanning. Wind and turbulence is problematic for stability of the scanner and the network of tiepoint reflectors. As a result, tiepoint referencing and point cloud quality can decrease for a certain scan position. This leads to less accuracy among the LiDAR point clouds when that scan position is referenced and merged with other scanner locations. The LiDAR data itself is also subject to mismatching with data from other scan positions. Merged scans from different scan positions have uncertainties on the order of 3-6 cm. This represents the X, Y, Z standard deviation residuals of the mismatch between tiepoint reflectors identified from each scan position with the an overall tiepoint reflector list that is used for the entire project. The February 2009 dataset yielded the lowest standard deviations for each scan position. For Victory Road, the following standard deviations were calculated:

Scan Position 1 - 0.0354 m

Scan Position 2 - 0.0279 m

Scan Position 3 - 0.0389 m

Scan Position 4 - 0.0183 m

Scan Position 5 - 0.0201 m.

For Brandy Lake, the lowest standard deviations were from the November 2009 survey:

Scan Position 1 - 0.0437 m

Scan Position 2 - 0.0317 m

Scan Position 3 - 0.0333 m

Scan Position 4 - 0.0432 m

Post-processing of LiDAR point cloud data

TLS acquires terrain data at a high resolution and therefore includes data from objects such as vegetation, passing traffic, street signs, and other man made structures. These objects are erroneous in terms of creating a usable bare-Earth digital elevation model of the terrain. In addition, there are other artifacts that are not real-world objects but become incorporated into the LiDAR point clouds for various reasons. These points need to be filtered out as well. Therefore, a significant amount of post-processing of the LiDAR data is needed to create a usable surface model.

The LiDAR data gathered for Brandy Lake and Victory Road were reanalyzed within RiScan Pro. Merging datasets from each scan position is accomplished by referencing each point cloud to the network of tiepoint reflectors. Due to systematic errors within the instrument itself, there is some degree of mismatch within each different set of point cloud data. Therefore, to minimize these errors, several iterations of tiepoint referencing combinations are needed to produce the most accurate merged point cloud of data. The last task in RiScan Pro is to export the raw point cloud data which contains Easting, Northing, Elevation, and Intensity for each LiDAR data point.

The raw point cloud data from RiScan Pro was then imported into Bentley's Microstation software. Subsequently, TerraSolid's TerraScan & TerraModeler applications were loaded into Microstation. Microstation was primarily used to navigate around the dataset and to subset, clip, or filter data.

TerraScan is used to classify and filter the raw LiDAR data. Classifying the LiDAR data enables the user to differentiate between points that are representative of the

true ground surface, from points that represent other above-ground objects, such as telephone poles, vegetation, passing cars, etc (Figures 21 & 22).

The data were first imported into TerraScan. In areas of dense point cloud data (most commonly in close proximity to the scanner itself) or standing water, many artificial points are created below the ground or water surface. The standing water creates reflections of surrounding objects which the scanner interprets as real data and thus creates an upside-down mirrored point cloud of the object observed in the water reflection (Figure 23). When these Low Points are concentrated around the scanner, it is likely caused by a travel time miscalculation. Regardless, these Low Points are the first to be classified. There are several tools within TerraScan which facilitate this process. This is a manual classification step which consumes the most time.

Once the Low Points are classified, the remaining data are run through a filter. This filter is created by a Macro running under TerraScan, and is made up of a list of algorithms which analyze and classify the data. Depending on the terrain scanned, certain parameters within the Macro are adjusted to maximize its effectiveness. For the purposes of this project, the Macro uses only the geometric arrangement of the LiDAR points in the point cloud to conduct its filtering.

The most important routine within the Macro is the Ground routine. This routine builds the Ground point class based on the geometric arrangement of data points. In TerraScan, it is based on the Adaptive TIN model described by Axelsson (2000). The Brandy Lake and Victory Road project sites were filtered with the same Ground class tolerances. Within the Ground routine settings, there are four important parameters that are set. For the Brandy Lake and Victory Road, the terrain angle, which is the natural

slope of the terrain, was set at 89.0° because of the presence of man-made structures. If the project area did not contain any man-made features, structures, or vertical rock outcrops, the terrain angle would be set to a lower setting depending on the natural slope of the area. In other words, the terrain angle parameter is a setting which allows the Ground routine to be more efficient by accounting for vertical objects or surfaces as well as the natural slope. The iteration angle was set at 6.0° and the iteration distance was set at 1.5 m. The iteration angle is the angle above the adaptive TIN surface edge where points that lie outside of this angle are classified as Vegetation. The iteration distance is a vertical distance along the iteration angle that dictates how far the Ground routine will search (Figure 24) The iteration angle and distance tolerances are both fairly conservative settings. An iteration angle of greater than 6.0° allows potential for the Macro to include points that are not representative of the ground surface. Therefore, points that were reflected off of low vegetation could be included in the Ground class. The same logic applies for the iteration distance. A larger iteration distance would increase the chance that vegetation could be classified as Ground points. Finally, the parameter for lessening the Ground iterations was set at its lowest setting, 1.5 m. This was done to ensure data density across the project site but to reduce the number of Ground points in the immediate area of the scanner.

After the data are run through the Macro, the Ground point class was isolated from the other points. TerraModeler was then used to check for anomalous points in the Ground class. TerraModeler builds a TIN surface out of the points and is capable of displaying contour lines and hillshade images of the LiDAR data. Once the Ground class was checked for accuracy, the points were exported for use in ESRI's ArcGIS software.

DEM Creation

The interpolation functions in ArcMap proved to be the most effective way of creating a DEM surface of the data. In particular, the Radial Basis Function (RBF) was usually the best method for creating a DEM. This is because the RBF forces a DEM surface through each point. Therefore, edge artifacts and unrealistic spikes in the surface model are minimized. The RBF search parameters were set to interpolate with a neighborhood of 15 points with a variable search radius. The kernel function was set to the Spline with Tension option. The Geostastical tool in ArcMap also calculates RMS values for the error residuals of the RBF surface model. If the RMS values for the error residuals are greater than 10 cm, then the LiDAR point cloud is not very accurate and does not allow for a useful temporal interpretation of the LiDAR data. The end result is a DEM that represents a mean surface that fits through the LiDAR point data.

Topographic profiles of the LiDAR point data were imported into MATLAB to plot the time series of the LiDAR data across each sinkhole. To analyze the temporal component of the sinkhole data, three strips of profile data were picked: one west-east profile across the western margin of Brandy Lake, a west-east profile along US-50 at Victory Road, and finally a north-south profile along Victory Road across US-50.

With this methodology, we were able to analyze the geometric properties of each sinkhole. In particular, the magnitude of vertical subsidence, the horizontal width of each sinkhole, and the general shape of each subsidence feature. By gathering multiple datasets over an 18-month span for each sinkhole, any continued subsidence could be observed.

Figure 14:
The Riegl LMS-Z620 survey LiDAR scanner is pictured here at Victory Road. It is mounted on top of a tripod at each scan location. Controlling the scanner is accomplished through RiScan Pro software which is installed on the laptop mounted on the tripod.

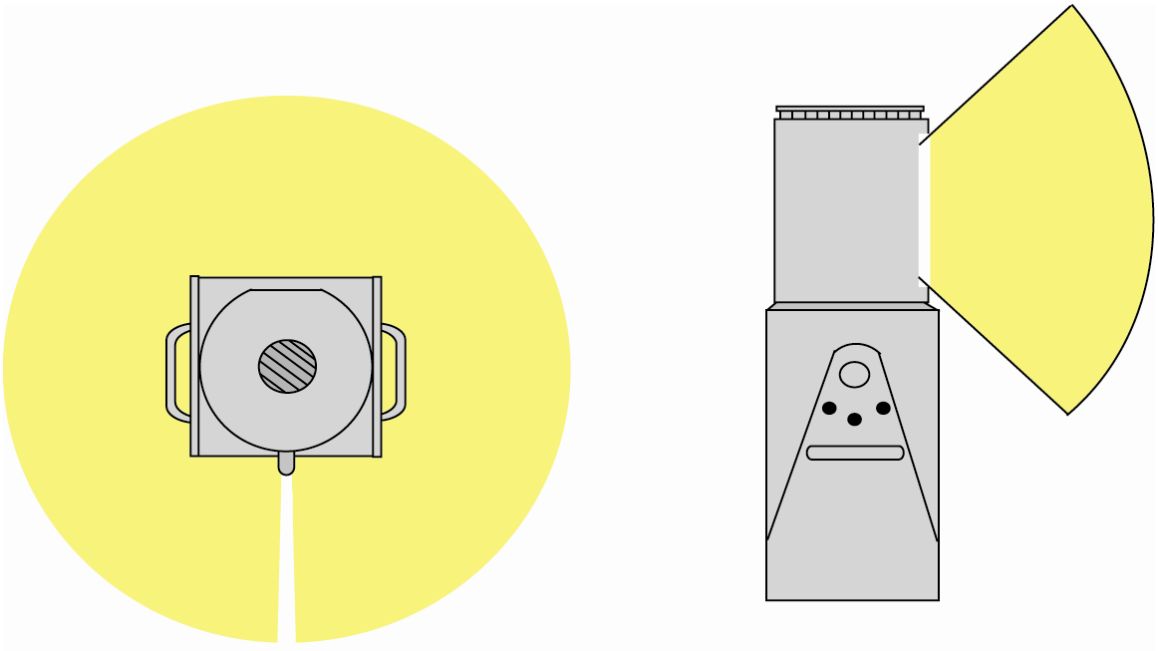

Figure 15:
The diagram on the left shows the LiDAR scanner in map view where it has a vertical axis range of nearly 360°. The diagram on the right shows a side profile view of the LiDAR scanner where it has a horizontal axis scanning range of 80°. The scanner can be tilted up or down to increase vertical data coverage.

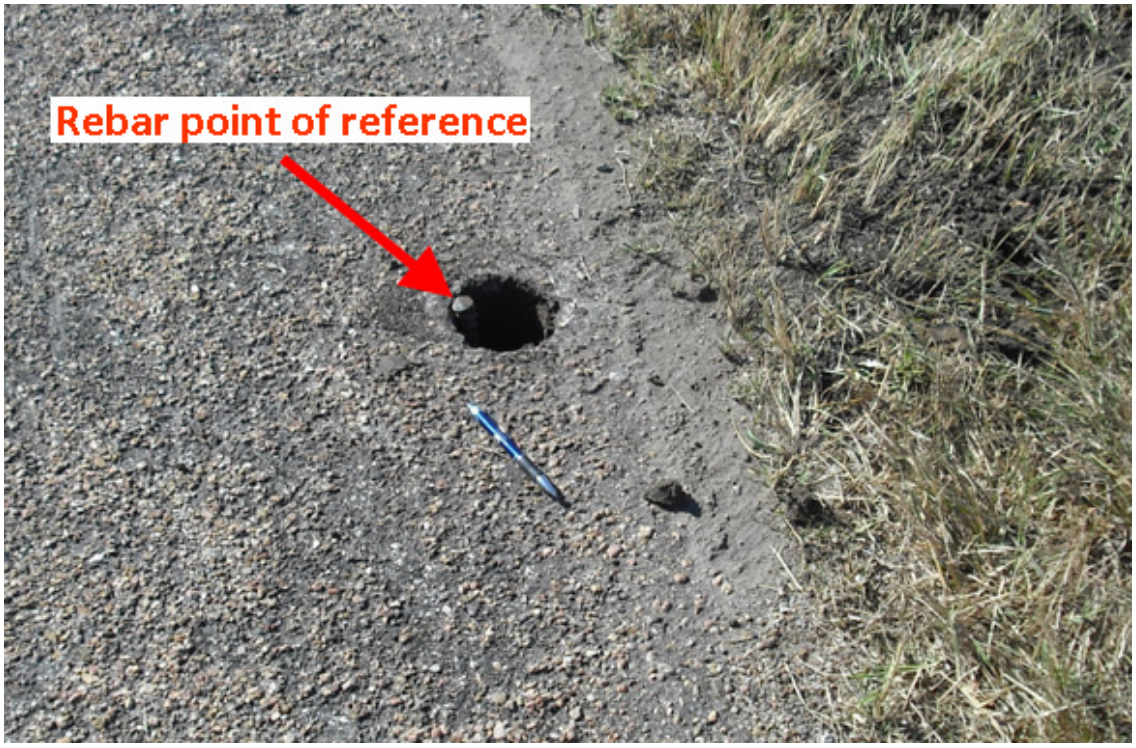

Figure 16:
At Brandy Lake and Victory Road, permanent monuments were placed near the edge of the road surface. An auger bit was drilled 2.0 m into the ground and then a rod of rebar was placed inside the hole with grout poured around it to set the rebar in place. A tiepoint reflector was placed over each monument location during successive scans.

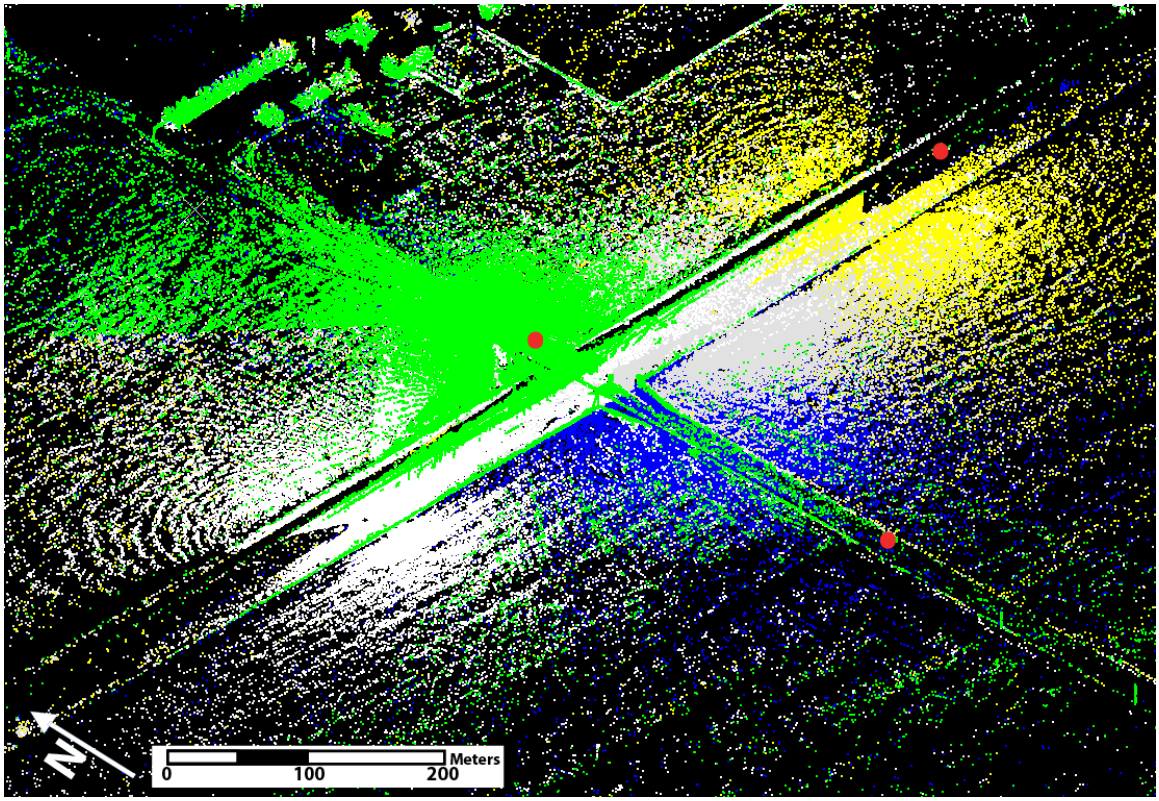

Figure 17:
A northeast looking bird's eye perspective of the November 2009 Victory Road LiDAR data set. The image is colored by each scan position gathered. Scan position 1-Blue, 2-Yellow, 3-Gray, 4-Green, 5-White. For the November 2009 survey, five scan positions were used to minimize data holes. The red markers indicated the locations of the permanent monuments that the data were referenced to.

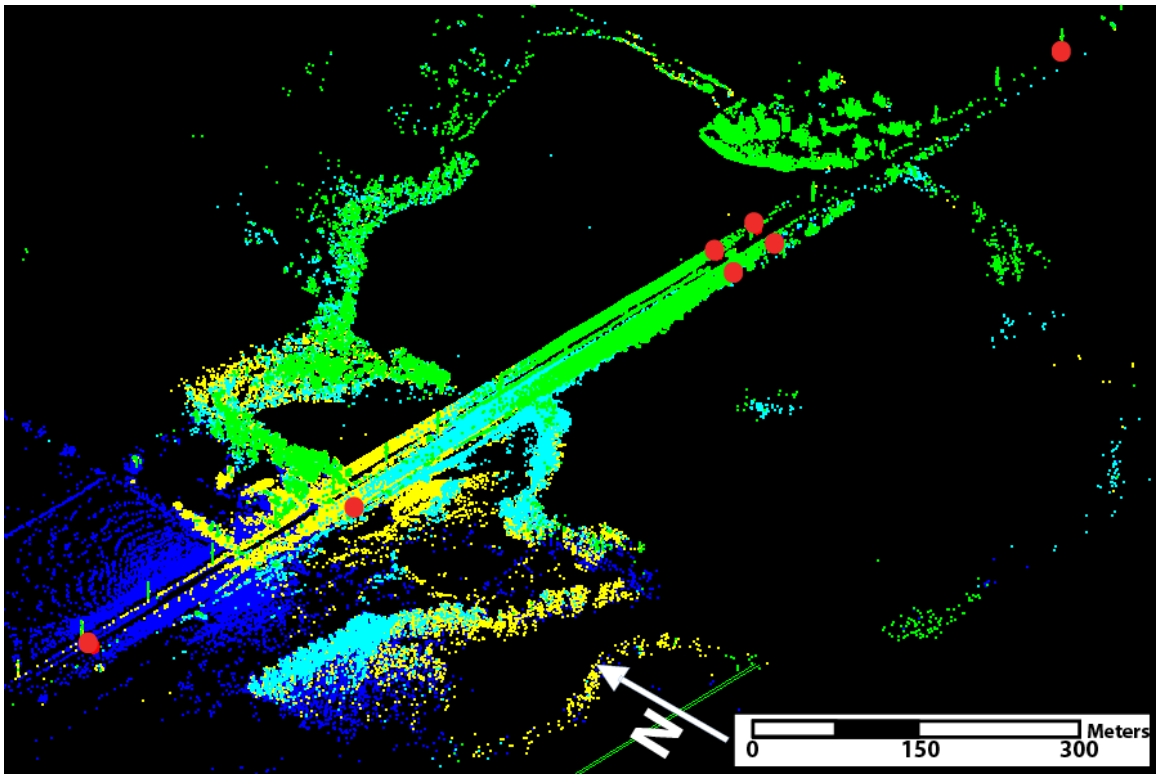

Figure 18:
A northeast looking bird's eye perspective of the Brandy Lake LiDAR data colored by each scan position. Scan position 1-Blue, 2-Yellow, 3-White, 4-Cyan, 5-Green. This is data from the November 2009 survey where only five scan position were needed. The red markers along US-50 indicate positions of the permanent monuments that the data were referenced to.

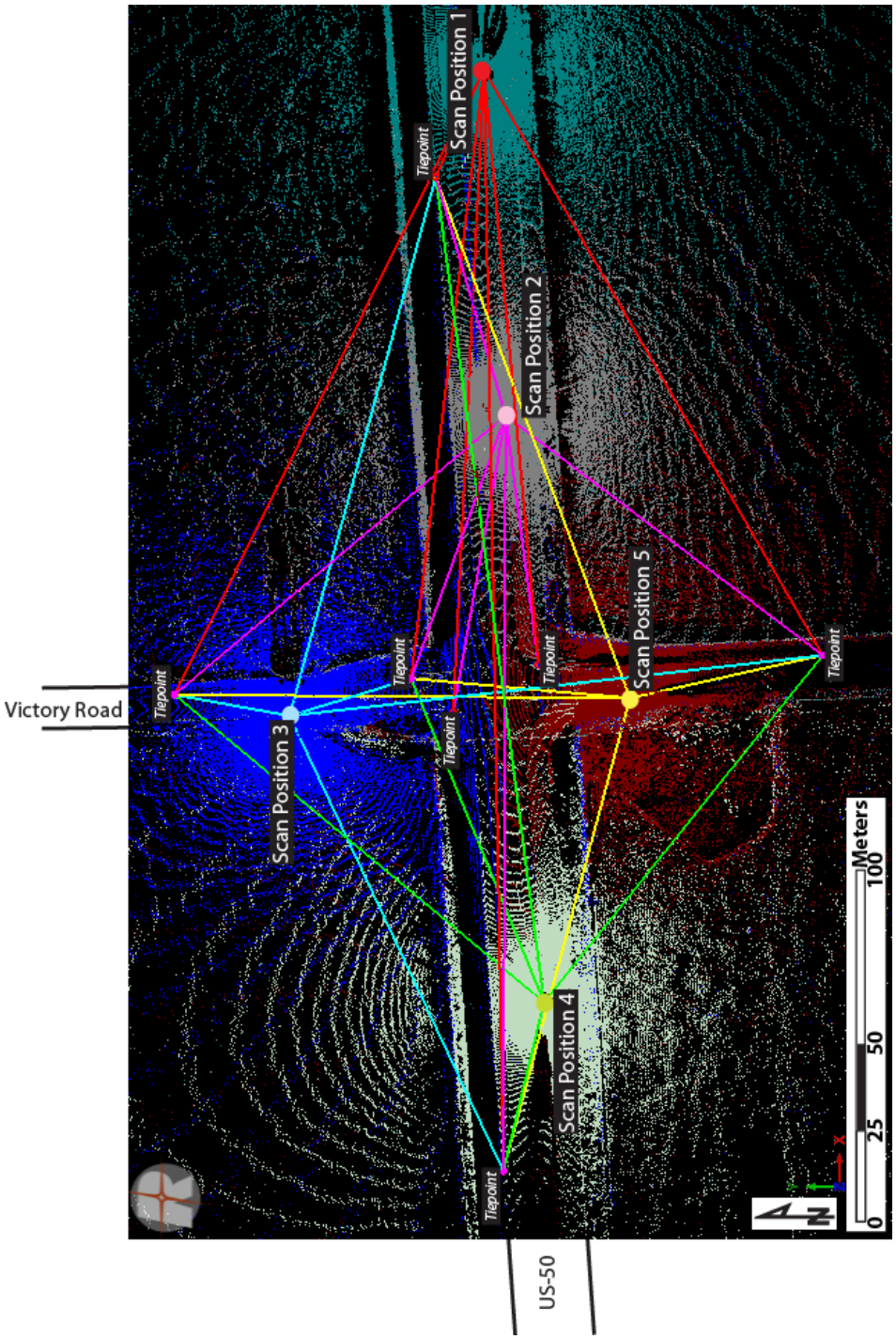

Figure 19:
A map view of the Victory Road/US-50 intersection LiDAR data with the data points colored by scan position to show the network of tiepoint reflectors relative to the scan positions. At each scan position, the tiepoints are fine scanned to resolve a more precise location. The lines from each Scan Position to each tiepoint indicate the look direction of the scanner to the tiepoint. Scan data are colored as follows: Scan Position 1-Teal, 2-Gray, 3-Blue, 4-White, 5- Maroon

Figure 20:
The Trimble 5800 RTK-GPS system gathers GPS coordinates of each monument location. It consists of a base station receiver (left tripod) that tracks satellite constellations. The rover receiver and data collector gather data relative to the base station. This is how it is able to attain accurate GPS coordinates.

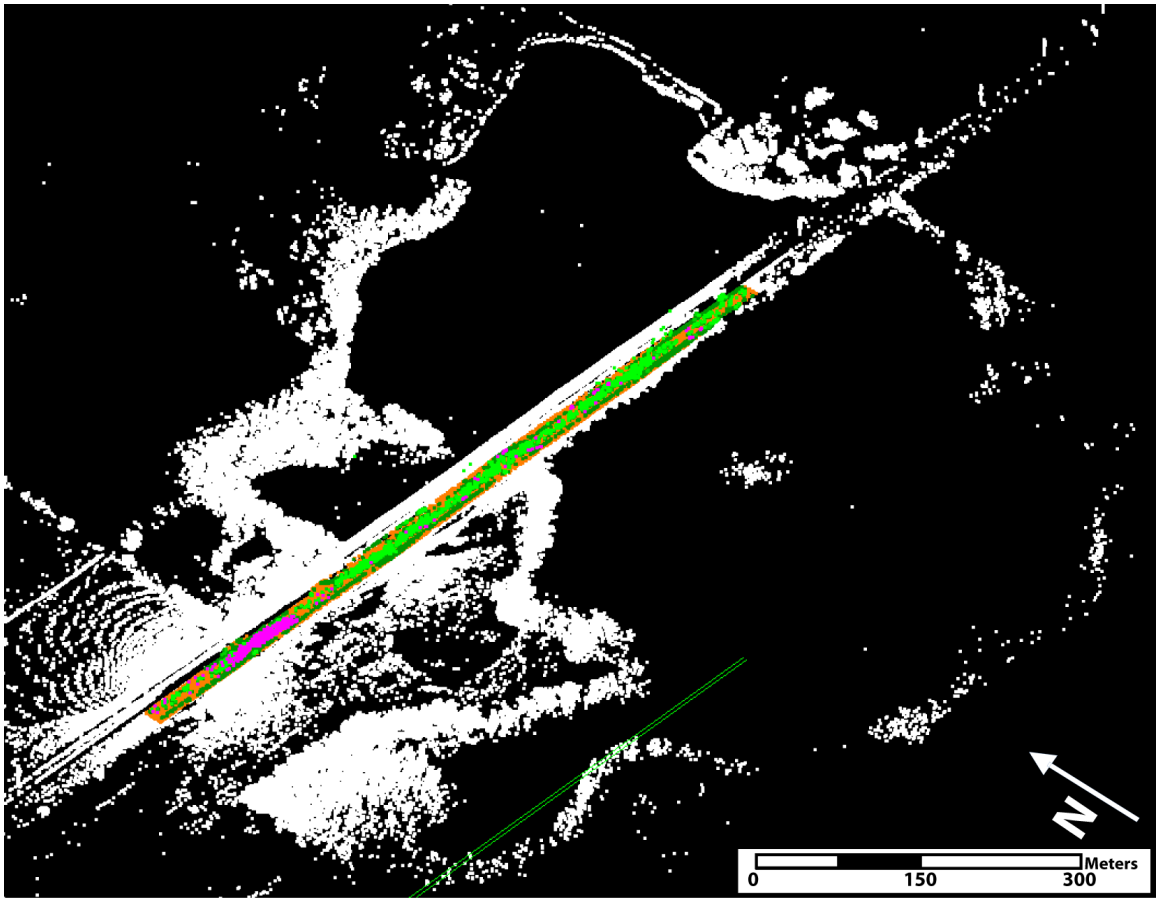

Figure 21:
The area of interest along US-50 was subset and filtered with the Macro from TerraScan and is shown as colors other than white. There are ~ 4,500,000 Ground points and ~1,000,000 points attributed to traffic noise and vegetation. The remaining ~20,000,000 points were left unclassified but still show the outline of the lake and surrounding area.

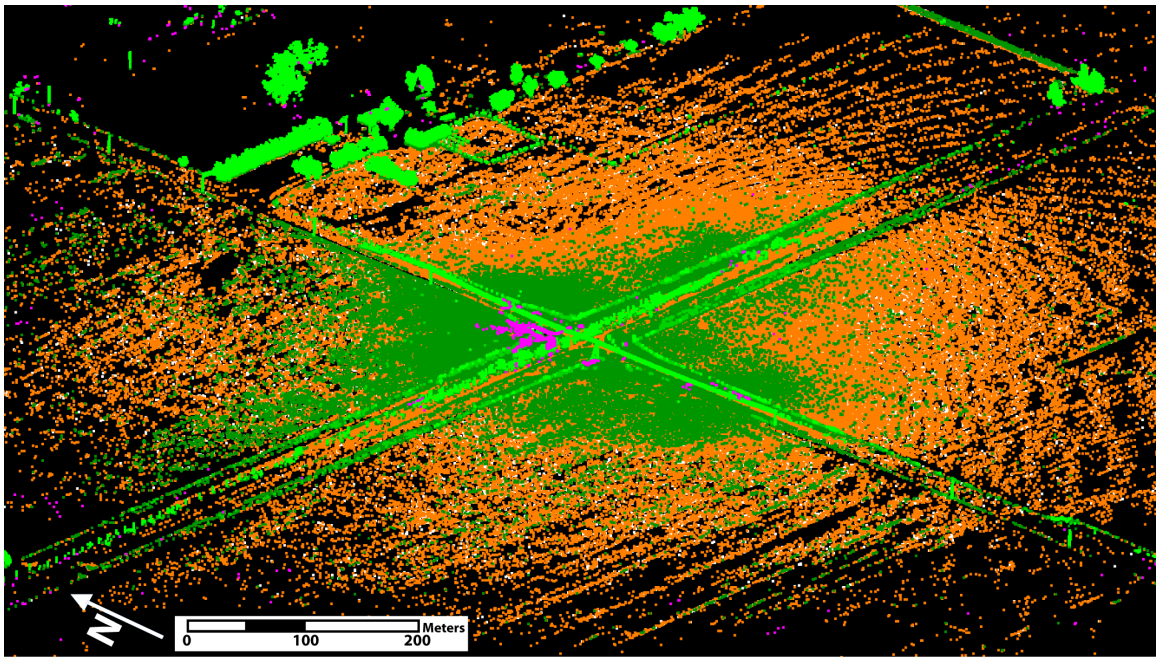

Figure 22:
The entire Victory Road dataset was filtered using TerraScan's Macro. The end result was ~1,000,000 Ground points and ~4,200,000 points classified as vegetation, traffic, or man-made structures. Approximately ~26,000 points that were manually classified as Low points. See text for discussion.

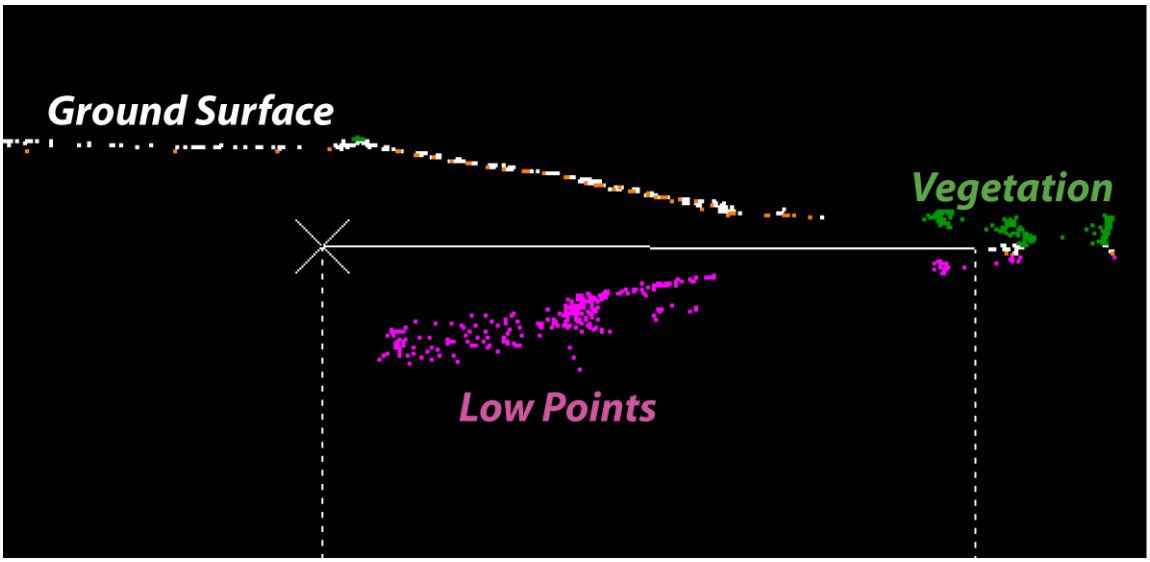

Figure 23:
Low points were manually classified by using a "Classify below line" tool in TerraScan. This was done by looking at vertical profile slices of the data and then using the tool to separate the Ground points from Low points. In the figure, Low points are colored fuchsia, while Ground points and Vegetation points are colored white and green respectively.

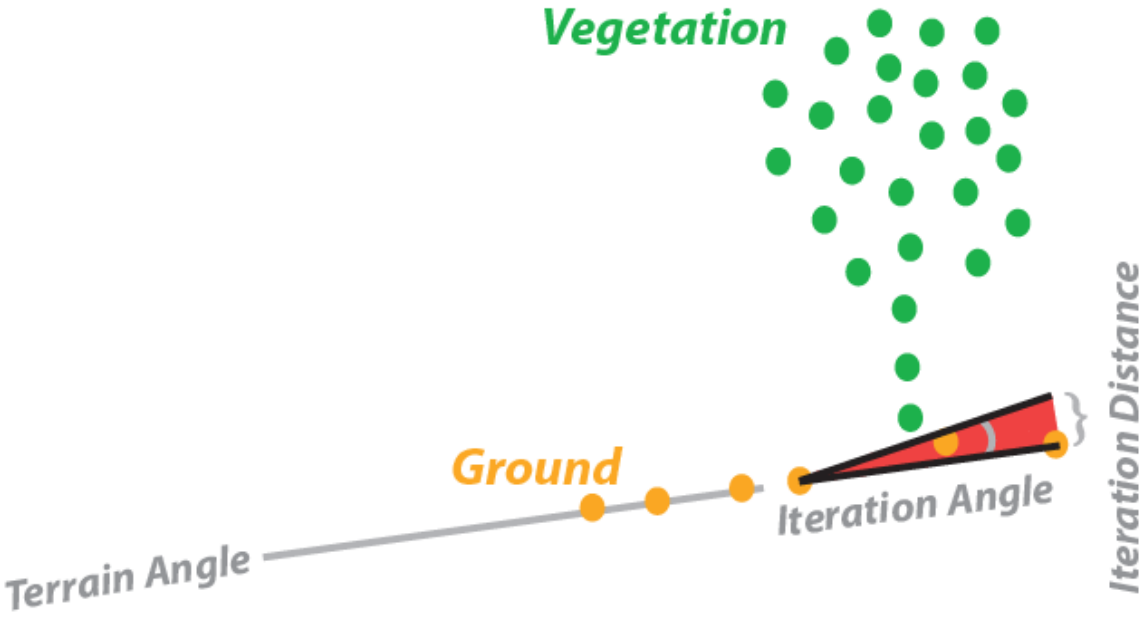

Figure 24:
Diagram of three Ground routine parameters in a TerraScan Macro. The Terrain Angle is set to follow the natural slope of ground surface. The Iteration Angle and Iteration Distance are search parameters which dictate what points are classified as Ground or Vegetation. The Iteration Angle is a search parameter that is the angle above the surface of a TIN edge that starts at a vertex point. The Iteration Distance is another search parameter that is the vertical distance along the Iteration Angle that dictates how far from the vertex point the Ground routine searches. The combination of the Iteration Angle and Iteration Distance produces a zone, displayed as red, where points are classified as Ground. Points outside of this zone are classified as Vegetation.

CHAPTER 3

Results

The TLS data of the Brandy Lake and Victory Road sinkholes cover a 13 month time span. The same areas of data were covered with each successive scanning survey to develop a time series in order to evaluate the evolution of surface subsidence. The following results of this study illustrate how the TLS method was used to delineate the geometry and spatial characteristics of the two sinkholes.

Brandy Lake

Qualitative Field Observations

Qualitative indicators of subsidence at Brandy Lake indicate recent activity since the construction of the US-50 roadway. These indicators are also the main reason for thorough data coverage along the western margin of the lake. The water level at Brandy Lake varies throughout the year, however along the western margin of the lake, there is significant ponding of water during the warmer months. This water encroaches to within a several feet of the roadway at its closest point (Figure 25).

Another qualitative observation is the presence or absence of wave benches along the roadway banks at certain points over the lake shorelines. Along the central and eastern sections of US-50 across Brandy Lake, there are noticeable, 30-35 cm high wave cuts in the banks of the road from wave action (Figure 26). These wave cuts are absent along the western sections of the roadway banks (Figure 27). Therefore, subsidence along the western section of the lake has been active and this is indicated by the temporal development of the wave cuts.

Fence lines along the north side of US-50 near the actively subsiding section are also submerged during the warmer seasons. The fenceposts are off plumb in this section where there is noticeable subsidence (Figure 27).

Brandy Lake LiDAR data

Analysis of the bare-Earth point cloud data reveals the nature of subsidence at Brandy Lake. The qualitative observations described above suggested that our LiDAR acquisition efforts be focused on the western margin of the lake.

In map view, a circular patch of tall grass was observed to the south of US-50 and west of Brandy Lake. This is an area where ponding of water occurs regularly and allows the tall, marsh grass to grow. This area is likely a recent sinking event that is related to subsidence that is occurring along the western margin of the lake and the dip along the surface of US-50.

The point cloud data over US-50 shows that subsidence manifests itself in a concave up depression along the western margin of the lake. However, this depression is noticeably asymmetrical. The deepest point of the actively sinking section is 1.15 m below the far field extrapolation outside of this section. This section at the road is 358 m long from the inflection points of subsidence along the road surface (Figure 28).

Data from Brandy Lake were gathered on February 2009, May 2009 and November 2009. A temporal analysis of these datasets reveals that there is virtually no change in the configuration of the road surface from the initial scanning survey to the most recent (Figure 29). The RMS error associated with the spread in the point cloud data from the November survey show a value of 0.0085 m across the length of the roadway from the cross validation result of the Radial Basis Function in ArcMap. The

standard deviations of the RTK-GPS points range from 0.09 cm to 2.2 cm in the X, Y and Z UTM coordinates. There is one anomalous elevation value that was gathered from the most eastern monument point which was 17.4 cm lower than average during the February survey. This is probably due to poor communication between the RTK-GPS rover receiver and base station at the time of acquisition. The effect of this anomalous point is likely the reason for the higher uncertainty in the February LiDAR point cloud which can be seen in Figure 29. However, within the errors associated with the GPS georeferencing and the LiDAR point cloud data, no subsidence over the observation period is interpreted along US-50 at Brandy Lake.

Victory Road

Qualitative Field Observations

Recent activity at the Victory Road sinkhole has caused qualitative indicators of subsidence. KDOT has resurfaced US-50 at Victory Road multiple times since the onset of subsidence. A resurfaced strip of US-50 can be seen from a 2002 orthophoto (Figure 10). In addition to the altered road surface, the west-east fence line north of US-50 and west of Victory Road dips down as it approaches the area of subsidence as well, indicating a significant amount of sinking.

Victory Road LiDAR data

Because of the noticeable water ponding and fence line sinking near the intersection of Victory Road and US-50, LiDAR acquisition was concentrated in this area. The subsidence that was first observed in the late 1990's is easily differentiable in the new the LiDAR data. The Victory Road sinkhole is 125 m wide from west to east

and is 117 m wide from north to south. Its magnitude of subsidence is 1.20 m (Figure 30). The RMS error of point cloud data from the November 2009 survey calculated from the Radial Basis Function in ArcMap was 0.0056 m. The center of maximum subsidence is also to the northwest of the Victory Road/US-50 intersection. Unlike at Brandy Lake, the Victory Road sinkhole has a characteristic bowl shaped geometry in map view. This is different from the asymmetric Brandy Lake site (Figure 31). Since this sinkhole has been recently repaved since the late 1990's a significant amount of relief has developed along the north and south margins of US-50. To compensate for this steep drop off from the asphalt, the Reno County road department filled part of the sinkhole to the north of US-50. This increase in elevation because of the road fill is seen in a north-south profile of the road (Figure 32). The total amount of fill that was put in elevated this part of Victory Road by 18 cm. The uncertainties associated with georeferencing from the RTK-GPS range from 0.006 cm to 3.5 cm in X, Y and Z UTM coordinates.

Each successive scan that was gathered over the Victory Road sinkhole yields little change in the geometry of the area over the course of the study. Similar to Brandy Lake, no active subsidence is observed in the area.

Figure 25:
A south looking photo taken from the south side of US-50 at the western margin of Brandy Lake. During warm months the water level from Brandy Lake encroaches into the ditches of US-50 along the western margin of the lake. This occurs near the subsided section of the road. See Figure 28 for location.

Figure 26:
A southwest looking photo along the fenceline on the north side of US-50. The development of wave benches in this central section of the road bank suggests that subsidence is inactive in areas east of the western margin of the lake. See Figure 28 for location.

Figure 27:
A north looking photo taken from the south side of US-50 at the western margin of Brandy Lake. The water level of the lake has submerged the fence line along the north side of the road. Some of the fence posts are off plumb as well. Also notice the absence of a well defined wave cut bench in the subsided bank of the road. See Figure 28 for location.

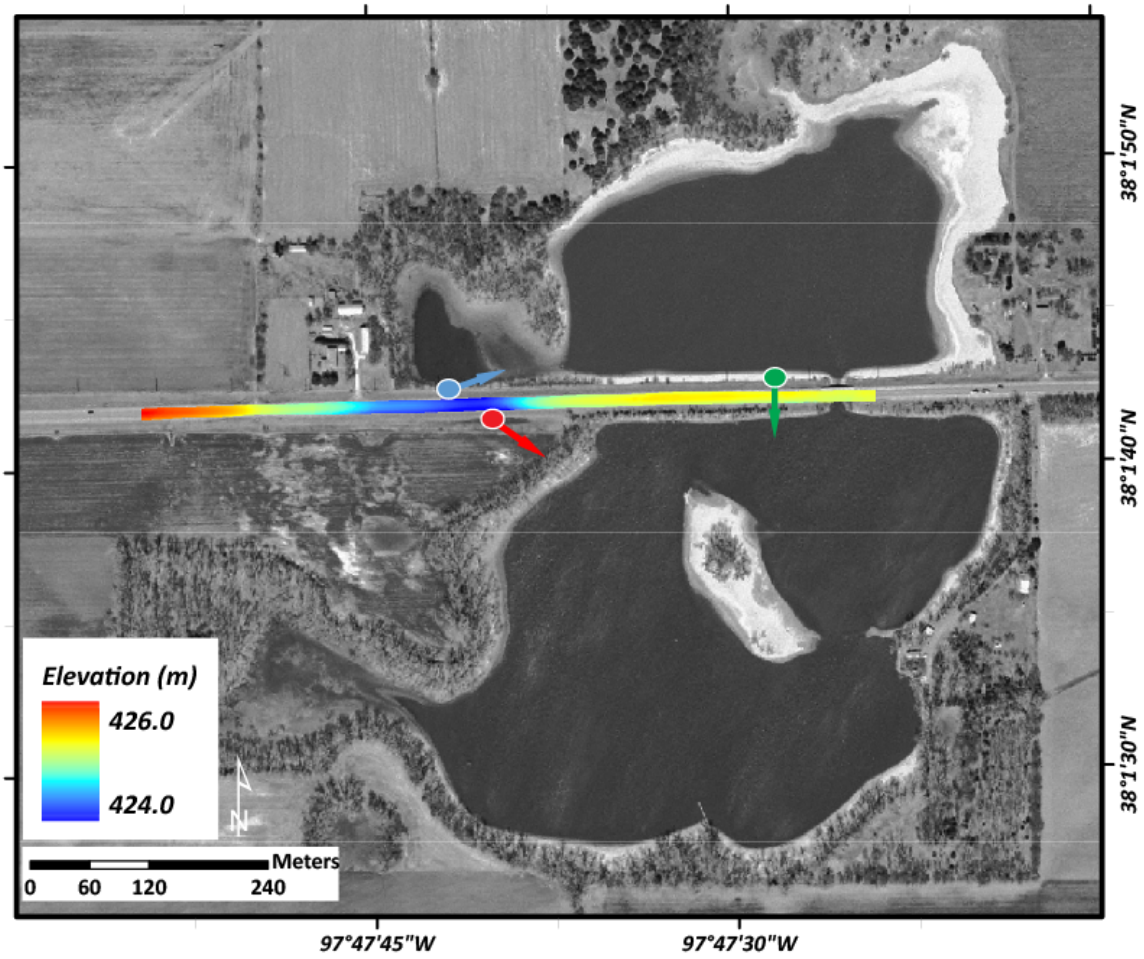

Figure 28:
The section of US-50 that was filtered in TerraScan was made into a surface model using ArcMap. This surface yields the map-view geometry of the active subsidence relative to the rest of the lake. The maximum point of subsidence is along the western margin of the lake, shown in blue. The location of Figure 25 is shown by the red marker, Figure 26 by the green marker, and Figure 27 is shown by the blue marker.

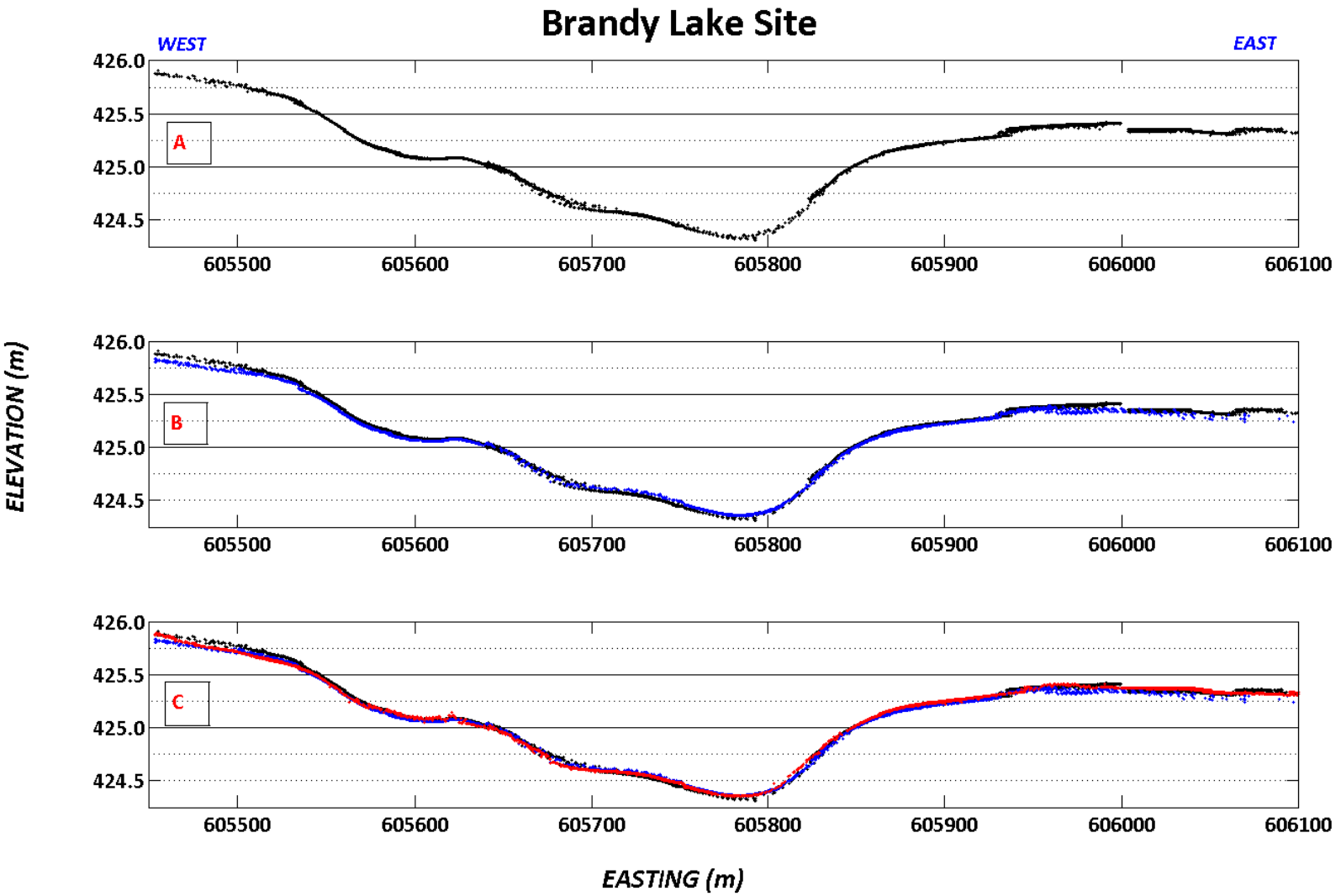
Brandy Lake Site
WEST
EAST
426.0
425.5
425.0
424.5
A
B
C
605500
605600
605700
605800
605900
606000
606100
ELEVATION (m)
EASTING (m)

Figure 29 (previous page):
A west-east profile along the centerline of US-50 at Brandy Lake shows the three datasets that were gathered along the western margin of the lake. A-Black-February 2009, B-Blue-May 2009, C-Red-November 2009. Within the error of the point cloud data, no active change in the road surface is observed. However, the point of maximum subsidence yields a magnitude of 1.15 m of sinking. Also, the subsidence along US-50 displays a unique asymmetric geometry where a "step" in subsidence is seen. The vertical exaggeration is 60x.

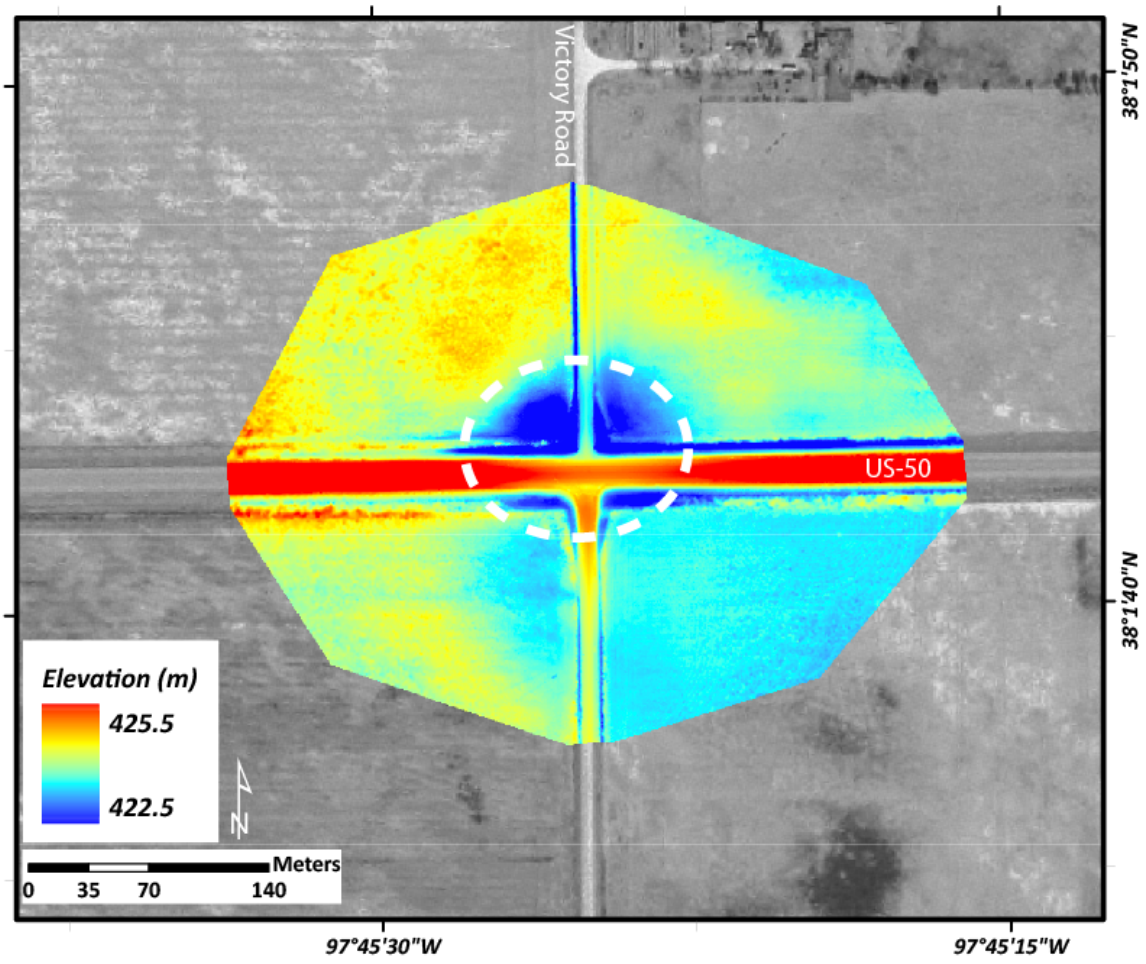

Figure 30:
DEM of the sinkhole at Victory Road that is underlain by an orthophoto shows the extent of the active sinkhole near the intersection. It takes on a symmetrical bowl-shaped geometry with a west-east diameter of 125 m and a north-south diameter of 117 m. The magnitude of subsidence of 1.20 m. The extent of the sinkhole is outlined in white.

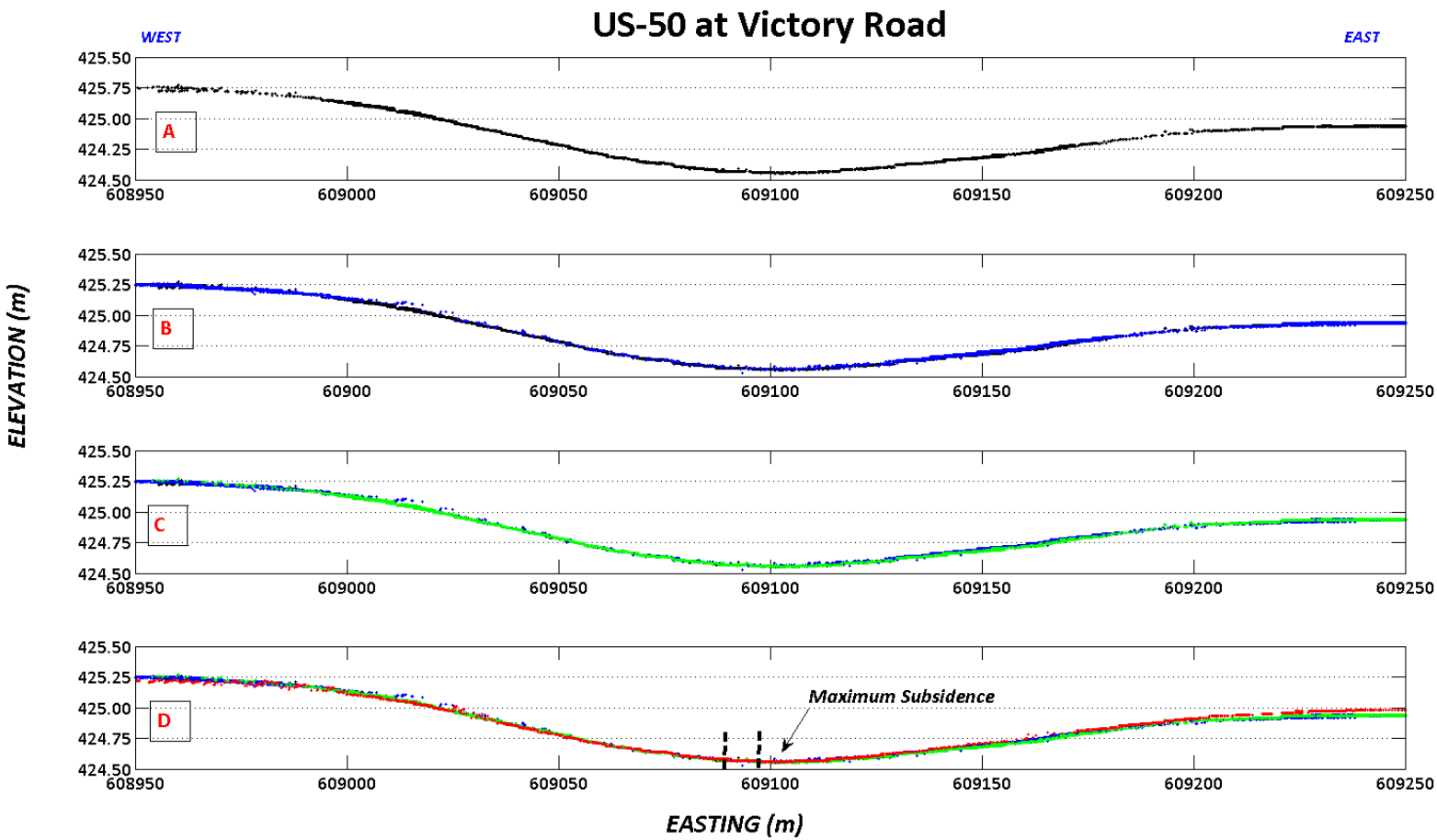
US-50 at Victory Road
WEST
EAST
A
B
C
D
425.50
425.75
425.25
425.00
424.75
424.50
608950
609000
609050
609100
609150
609200
609250
Maximum Subsidence
ELEVATION (m)
EASTING (m)

Figure 31 (previous page):
A west-east profile along the centerline of US-50 at Victory Road shows that there has been no active change in the road surface for the duration of this study. The datasets are colored by date: A-October 2008-Black, B-February 2009-Cyan, C-May 2009-Green, D-November 2009-Red. The profile also shows the bowl-shaped geometry of the subsidence feature. The dashed vertical lines show where Victory Road crosses US-50, the vertical exaggeration is 30x.

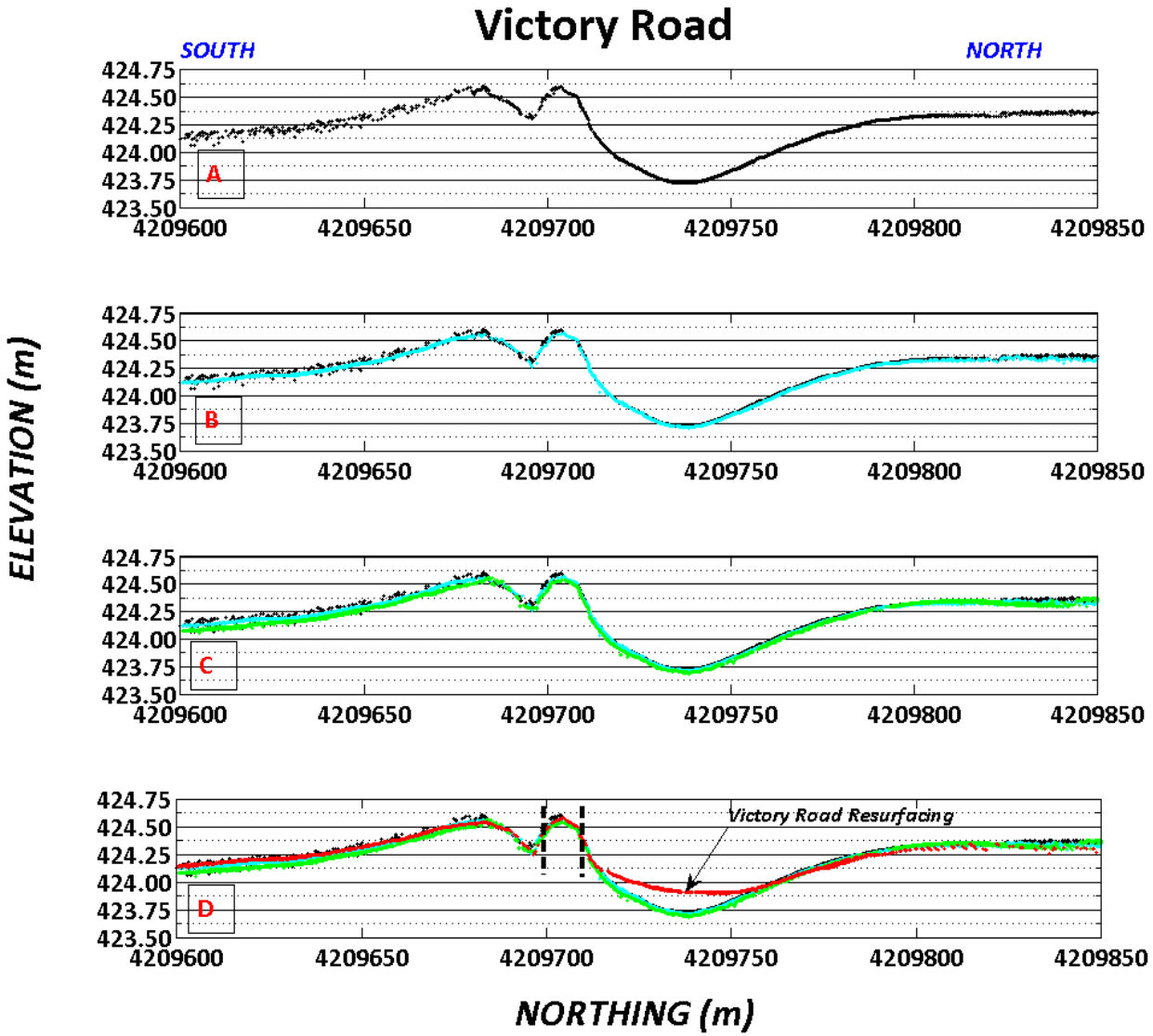
Victory Road
SOUTH
NORTH
424.75
424.50
424.25
424.00
423.75
423.50
A
B
C
D
4209600
4209650
4209700
4209750
4209800
4209850
Victory Road Resurfacing
ELEVATION (m)
NORTHING (m)

Figure 32 (previous page):
A north-south profile along the center of Victory Road shows where the maximum point of subsidence is relative to US-50. The datasets are colored by date: A-October 2008-Black, B-February 2009-Cyan, C-May 2009-Green, D-November 2009-Red. The latest scanning survey shows where the infilling of Victory Road north of US-50 took place. The fill is up to 18 cm in the deepest part of the sinkhole. If the fill is not taken into account, no active change in the road surface is seen. The dashed lines show where the margins of US-50 are. The margins of US-50 where the asphalt ends are points of significant relief as evidenced by the dip along the south side of the highway when transitioning to the gravel that makes up Victory Road.

CHAPTER 4

Discussion

Interpretation of Results

Subsurface mapping of the Hutchinson Salt Member (Walters, 1978; Watney, 1980; Watney & Nissen, 2004) shows the regional configuration of the salt across Reno County, Kansas. In addition, studies from Xia et al. (1995) and Anderson et al. (1994) detail the presence of subsurface faulting of the overlying Permian strata. The presence of a naturally occurring dissolution front also contributes to subsurface karsting and surface subsidence. This is an active phenomenon which has deformed the road surface of US-50. However, the results of this study indicate no significant subsidence is observed using LiDAR data spanning a time interval from October 2008 - November 2009 for both the Brandy Lake and Victory Road sites. This has implications for understanding the spatial development of subsidence features from natural dissolution of subsurface salt.

From the LiDAR profile, the geometry of the Brandy Lake sinkhole presents an interest find. From the profile data extracted along the western margin of Brandy Lake on US-50, a noticeable step in the elevations is observed. This could be due to episodic dissolution events where the subsidence of greatest magnitude and wavelength in the eastern part of the active sink occurred first. Subsequently, another subsidence event expanded the original deformation area further to the west. These observations are consistent with a model of episodic westward dissolution as originally proposed by Anderson et al. (1994).

At Victory Road, a lack of subsidence over the time span of observation for this study is quite different from the observations of the Kansas Department of Transportation in the late 1990's. In that study, which began in October 1998, a subsidence rate of 0.25 m/yr of subsidence was determined at Victory Road at the onset of surface subsidence (Rice, 2009). Within 10 years from the time of the KDOT observations to the time of this study, subsidence appears quiescent over the time span of our observations and within the detection limits of the LiDAR data. This suggests that naturally occurring subsidence features in south-central Kansas can initiate relatively rapidly and continue for a few years, followed by periods of inactivity Evidence for transient deformation episodes in the past are based on paleosubsidence features detected through seismic methods (Miller & Xia (2002); active subsidence detected by KDOT at Victory Road in 1998 (Rice, 2009), and the current inactivity at the same site and within the detection limits of our data. This alternating behavior of active subsidence followed by periods of quiescence may result from episodic leaching of the Hutchinson Salt at depth.

The paleosubsidence features have been mapped out by Miller & Xia (2002) suggests past leaching of the salt at Victory Road. This observation is consistent with episodic surface subsidence at the local scale. Although subsidence features have regionally formed along the main dissolution front and along other structural features such as the Arkansas River Lineament, locally, these sinkholes are isolated features that can be reactivated depending on the amount of subsurface karsting controlled by the distribution of shallower, small scale faults observed in the seismic data. The initiation of the paleosinkholes at Brandy Lake is unknown while sinkholes at Victory Road have occurred since the Tertiary (Miller & Xia, 2002).

A model for the advancement of the dissolution front proposed by Anderson et al. (1994) described the leaching of the Hutchinson Salt through time and how the distribution of subsurface fractures affect surface subsidence and infill (Figure 33). This model agrees with observations from seismic studies where episodes of subsidence and deposition of sediments result from the dissolution of the salt at depth. From the interpretation of the LiDAR data from this study, these episodes of subsidence are likely smaller sinkholes that locally form quickly and are relatively small compared to the broader dissolution front in Reno County. Furthermore, the small scale infill features from Anderson et al.'s (1994) block diagram model can also be asymmetric or bow-shaped in cross section as implied by the surface expression of the two sinkholes in this study.

Precipitation

The initiation of subsidence is not a well understood process. Intuitively, a large influx of precipitation could cause subsidence to initiate for a given area. However, this process is likely more complex than a simple cause and effect relationship.

For example, active subsidence has been documented in areas of Spain where evaporite leaching is occurring (Soriano & Simon, 2002). In that study, active subsidence of sinkholes is quantified and a rate is measured. Precipitation that occurred during the same time as the sinking was analyzed in an attempt to correlate major rainfall events or high precipitation periods with subsidence. However, no correlation exists between precipitation and active subsidence that is taking place. Guerrero et al. (2008)

also suggest that individual sinkhole events occur randomly and are difficult to predict on a short timescale.

In this study, precipitation data were gathered for the Hutchinson area and plotted against the subsidence data gathered from KDOT starting in 1998 at the onset of Victory Road subsidence. Similar to the study conducted by Soriano & Simon (2002), there is no obvious correlation between rainfall peaks and the onset of subsidence (Figure 34). However, because of the nature of dissolution and subsidence in Reno County, precipitation and subsidence may be anti-correlated. This is due to the fact that there are many variables which connect an influx of undersaturated water with ground subsidence. First, precipitated rain water must infiltrate down to the salt, possibly via fractures in the subsurface. Enough of the salt must be leached to create overburden stress in the overlying strata (Miller & Xia, 2002). Once the overburden stress exceeds the yield strength of the overlying strata, subsidence can occur. This process suggests that there is a significant amount of lag time between precipitation and subsidence.

Implications

The initial use of terrestrial LiDAR to image actively deforming sinkholes has provided a means to accurately delineate their lateral extent. Interpreting the internal geometry of the sinkholes is also facilitated by the use of LiDAR in creating detailed digital elevation models. At Brandy Lake, the noticeable "step" in the subsidence shape along the western margin of the lake raises questions about the timing and nature of subsidence in the area. Continued monitoring of these two features is warranted because of the accuracy in measuring the magnitude of strain at US-50. Similar studies are

possible on actively deforming surface features that are in different settings such as fields and other natural landscapes. However, natural landscapes are subject to alterations by surface processes (i.e. swelling of soils, erosion of the landscape) and by farming practices, so the ability to track deformation of the Earth's surface could prove more challenging.

This study provides an approach where future studies of sinkhole evolution can be compared to. If subsidence at Victory Road is characteristic of natural subsidence in general in south-central Kansas, then that would indicate that sinkhole monitoring should begin immediately at the onset of deformation since these phenomena may not continue for more than a couple of years. Regardless, with future monitoring of sinkhole development in south-central Kansas, a better understanding of the subsurface karsting process can be attained.

Finally, this remote sensing technique also demonstrates the capabilities of terrestrial laser scanning in geomorphic investigations. This study helps in establishing a coherent workflow for the use of TLS in geologic applications. The inherent systematic error in the scanner itself, as well as the errors associated with the georeferencing techniques was sufficient enough to image any change (due to the infill of the Victory Road sinkhole) or lack thereof.

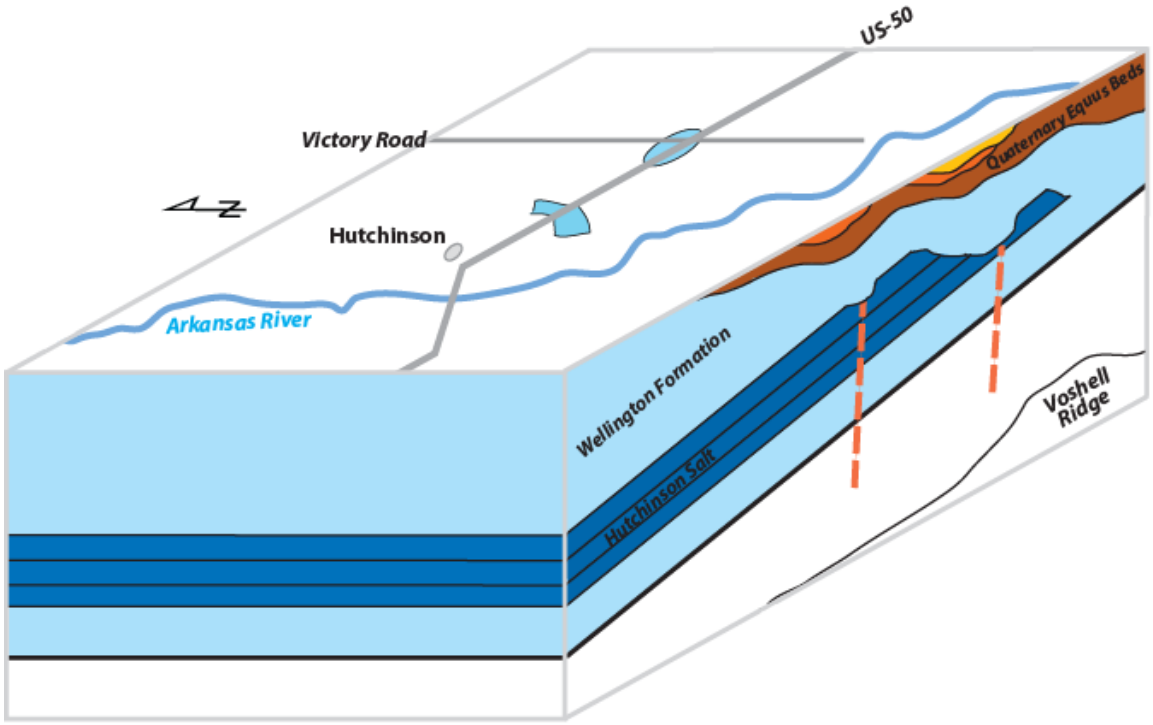

Figure 33:
A block model diagram with a northeast looking perspective with which shows the Voshell Ridge at depth along with the nature of the Hutchinson Salt Member in eastern Reno County. The concept of a block model for subsurface dissolution correlates with the results of this study. Anderson et al. (1994) proposed a model where episodic dissolution of the salt along fracture lineaments can lead to sinkholes with infill of quaternary deposits. The sinkholes in this study could be along a preferential dissolution zone whereby episodes of subsidence are initiated by rapid dissolution at depth.

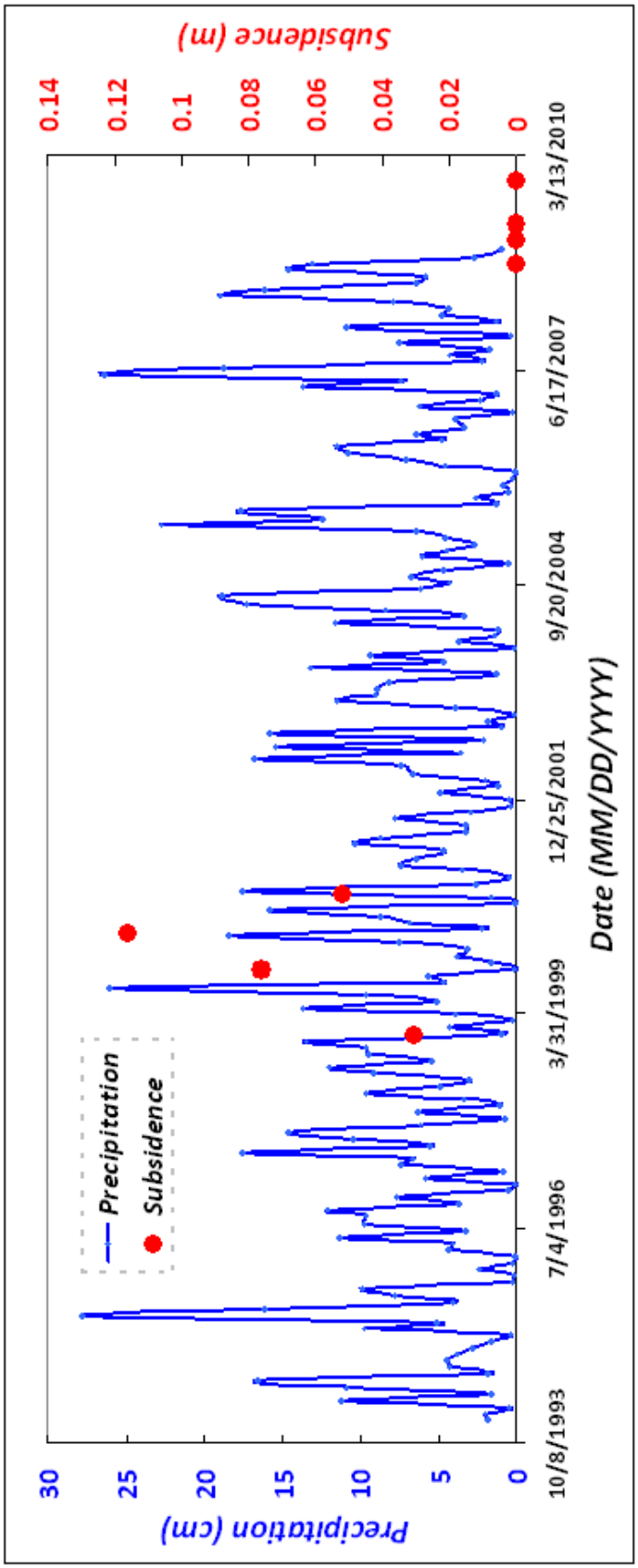
Subsidence (m)
0.14
0.12
0.1
0.08
0.06
0.04
0.02
0
Precipitation (cm)
30
25
20
15
10
5
0
Precipitation
Subsidence
10/8/1993
7/4/1996
3/31/1999
12/25/2001
9/20/2004
6/17/2007
3/13/2010
Date (MM/DD/YYYY)

Figure 34 (previous page):
A compilation of precipitation data for Hutchinson overlain on subsidence data gathered by KDOT and this study over the last 15 years. The data show a lack of correlation between rapid subsidence at Victory Road with any significant rainfall event that occurred during the same time. The onset of rapid subsidence at Victory Road is not understood well enough to correlate to precipitation patterns.

References

Abelson, M., Baer, G., Shtivelman, V., Wachs, D., Raz, E., Crouvi, O., Kurzon, I. & Yechieli, Y., 2003, Collapse-sinkholes and radar interferomety reveal neotectonics concealed within the Dead Sea basin: Geophysical Research Letters, v. 30;10

Anderson, N. & Knapp, R., 1993, An overview of some of the large scale mechanisms of salt dissolution in western Canada: Geophysics, v. 58;9, p. 1375-1387

Anderson, N., Hopkins, J., Martinez, A., Knapp, R., Macfarlane, P.A. Watney, W.L. & Black, R., 1994, Dissolution of Bedded Rock Salt: A Seismic Profile across the active eastern margin of the Hutchinson Salt Member, Central Kansas: Computers & Geosciences, v. 20;5, p. 889-903

Anderson, N., Martinez, A., Hopkins, J. & Carr, T., 1998, Salt dissolution and surface subsidence in central Kansas: A seismic investigation of the anthropogenic and natural origin models: Geophysics, v. 63; 3, p. 366-378

Axelsson, P., 2000, DEM Generation from Laser Scanner Data using Adaptive TIN Models: International archives of photogrammetry and remote sensing, v. 33;Part B4/1;Part4, p. 110-117

Baer, G., Schattner, U., Wachs, D., Sandwell, D., Wdowinski, S. & Frydman, S., 2002, The lowest place on Earth is subsiding- An InSAR (interferometric synthetic aperture radar) perspective: Geological Society of American Bulletin, v. 114;1, p. 12-23

Bellian, J., Kerans, C. & Jennette, D., 2005, Digital outcrop models; applications of terrestrial scanning lidar technology in stratigraphic modeling: Journal of Sedimentary Research, v. 75;2, p. 166-176

Cole, V.B., 1976, Configuration of the top of Precambrian rocks in Kansas: Kansas Geological Survey, Map M-7, scale 1:500,000

Closson, D., 2005, Structural control of sinkholes and subsidence hazards along the Jordanian Dead Sea coast: Environmental Geology, v. 47, p. 290-301

Closson, D., Karaki, N.A., Klinger, Y. & Hussein, M.J., 2005, Subsidence and Sinkhole Hazard Assessment in the Southern Dead Sea Area, Jordan: Pure and Applied Geophysics, v. 162, p. 221-248

Croxton, N., 2002, Subsidence on I-70 in Russell County, Kansas Related to Salt Dissolution- A History: The Professional Geologist, v. 39;8 p. 2-7

Galve, J.P., Gutierrez, F., Lucha, P., Bonachea, J., Remondo, J., Cendrero, A., Gutierrez, M., Gimeno, M.J., Pardo, G. & Sanchez, J.A., 2009, Sinkholes in the salt-bearing evaporite karst of Ebro River valley upstream of Zaragoza city (NE Spain) Geomorphological mapping and analysis as a basis for risk management: Geomorphology, v. 108, p. 145-158

Guerrero, J., Gutierrez, F. & Lucha, P., 2004, Paleosubsidence and active subsidence due to evaporite dissolution in the Zaragoza area (Huerva River valley, NE Spain): processes, spatial distribution and protection measures for transport routes: Engineering Geology, v. 72, p. 309-329

Gutierrez, F., Calaforra, J.M., Cardona, F., Orti, F., Duran, J.J. & Garay, P., 2008, Geological and environmental implications of the evaporite karst in Spain: Environmental Geology, v. 53, p. 951-965

Gutierrez, F., Cooper, A.H. & Johnson, K.S., 2008, Identification, prediction, and mitigation of sinkhole hazards in evaporite karst areas: Environmental Geology, v. 53, p. 1007-1022

Gutierrez, F., Guerrero, J. & Lucha, P., 2008, Quantitative sinkhole hazard assessment. A case study from the Ebro Valley evaporite alluvial karst (NE Spain): Natural Hazards, v. 45, p. 211-233

Gutierrez, F., Guerrero, J. & Lucha, P., 2008, A genetic classification of sinkholes illustrated from evaporite paleokarst exposure in Spain: Environmental Geology, v. 53, p. 993-1006

Kruger, J., 1996, Gravity and Magnetic Maps of Kansas: Kansas Geological Survey Open-File Report, v. 51

Lane, C. & Miller, D., 1965, Geohydrology of Sedgwick County, Kansas: Kansas Geological Survey Bulletin, v. 176, p.

Merriam, D.F., 1963, The Geological History of Kansas: Kansas Geological Survey Bulletin, v. 162, p. 1-317

Miller, R. & Xia, J., 2002, High Resolution Seismic Reflection Investigation of a Subsidence feature on U.S. Highway 50 near Hutchinson, Kansas: Proceedings Symposium on the Application of Geophysics to Engineering and Environmental Problems SAGEEP, p. 13CAV6

Miller, R., Xia, J. & Steeples, D., 2009, Seismic Reflection Characteristics of Naturally-Induced Subsidence Affecting Transportation: Journal of Earth Sciences, v. 20;3, p. 496-512

Nagihara, S., 2006, Use of Ground-Based LiDAR in Geomorphic and Surface Stratigraphic Studies: Gulf Coast Association of Geological Societies Transactions, v. 56, p. 659-664

Nissen, S. & Watney, W.L., 2004, Detailed mapping of the Upper Hutchinson Salt and Overlying Permian strata beneath Hutchinson, Kansas: Kansas Geological Survey Open-File Report, v. 2003;66

Rice, D., 2009, Applicability of 2-D Time-Lapse High-Resolution Seismic Reflection Approach to Image Natural Salt-Dissolution and Subsidence in Central Kansas and Improved Post-Processed Vibroseis Data Characteristics [M.S. Thesis]: Lawrence, University of Kansas

Seale, L., Florea, L., Vacher, H. and Brinkmann, R., 2008, Using ALSM to map sinkholes in the urbanized covered karst of Pinellas County, Florida-1, methodological considerations: Environmental Geology, v. 54, p. 995-1005

Shrestha, R. L., Carter, W. E., Lee, M., Finer, P. and Sartori, M., 1999, Airborne Laser Swath Mapping: Accuracy assessment for surveying and mapping applications: Surveying and Land Information Systems Journal of the American Congress on Surveying and Mapping, v. 59; 2, p. 83-94

Soriano, M.A. & Simon, J. L., 1995, Alluvial dolines in the central Ebro basin, Spain: a spatial and developmental hazard analysis: Geomorphology, v. 11, p. 295-309

Soriano, M.A. & Simon, J.L., 2002, Subsidence rates and urban damages in alluvial dolines of the Central Ebro basin (NE Spain): Environmental Geology, v. 42, p. 476-484

Steeples, D., Knapp, R. & McElwee, C., 1986, Seismic reflection investigations of sinkholes beneath Interstate 70 in Kansas: Geophysics, v. 51;2, p. 295-301

Tarolli, P., Arrowsmith, J.R. & Vivoni, E., 2009, Understanding earth surface processes from remotely sensed digital terrain models: Geomorphology, v. 113, p. 1-3

Walters, R., 1978, Land Subsidence in Central Kansas related to salt dissolution: Kansas Geological Survey Bulletin, v. 214

Waltham, T., 2008, Sinkhole hazard case histories in karst terrains: Quarterly Journal of Engineering Geology and Hydrogeology, v. 41, p. 291-300

Watney, W. L., 1980, Subsurface Geologic Study of the Hutchinson Salt: Kansas Geological Survey Open-File Report, 80-16

Watney, W. L. & Paul, S., 1980, Maps and Cross Sections of the Lower Permian Hutchinson Salt in Kansas: Kansas Geological Survey Open-File Report, 80-7

Xia, J., Miller, R.D., Steeples, D.W., and Adkins-Heljeson, D., 1995, Kansas Geological Survey Map Series, M-41E

Zeller, D., 1968, The Stratigraphic Succession in Kansas: Kansas Geological Survey Bulletin, v. 168

APPENDIX

LiDAR Workflow

1.) Planning

2.) Equipment Checklist for:

Riegl LMS-Z620

Trimble 5800 RTK-GPS

3.) Georeferencing Procedure

4.) Tiepoint Reflector Set Up

5.) LiDAR Scanner Set Up

6.) LiDAR Acquisition

7.) Post Processing

Microstation

TerraScan

TerraModeler

ArcMap

MATLAB

**Note-the following workflow is color coded to display "listed" items as green, "instructional" items as blue, and "command script" items as red*

1.) Planning

Prior to using the scanner, take careful attention to properly plan a scanning project.

Below are a few critical factors:

- Amount of area that should have data quality data coverage
- GPS control for georeferencing
- Weather restrictions
- Traffic
- General field supplies (i.e. water, food, sunblock etc.)
- All relevant scanning equipment
- Survey team

Area

Depending on your field area and what the project requires, the scanner has certain limitations. First of all, its range is specified to collect data up to 2.0 km away. However, data resolution and quality decrease with distance and it will not be capable of collecting up to sub-centimeter scale data at great distances. While keeping scanning resolution in mind, as well as the start and stop angles for each scan, budget enough time to acquire complete data. Consider maintaining uniform data coverage from scan position to scan position also.

GPS control

For merging a time series of scans or spatially constraining a project area relative to its surroundings, GPS control is needed. Therefore, set aside enough time to gather a minimum of 4 GPS control points, although more is recommended. This is most easily done with a Real Time Kinematic (RTK) GPS system to retrieve accurate GPS points. In most cases, this takes 1-3 hours.

Weather Restrictions

The scanner can operate in most temperature ranges (~0°-35°C) therefore this is not a critical factor. However, the camera mounted on top of the scanner must not be exposed to any amount of moisture. The scanner itself can be effectively operated in very light precipitation, however this is strongly discouraged. In addition, ponded water or any body of water is interpreted by the LiDAR scanner as no data/null areas. The presence of snow and ice in significant amounts may misrepresent an underlying surface or terrain.

Traffic

If the project area is an area of moderate to heavy traffic, safety is a priority. Also, in some cases, take action to mitigate vehicles blocking the view of the scanner. Although in-house processing subtracts vehicle noise, large trucks or semis can present a problem when the scanner attempts to detect (fine scan) far away reflectors or objects. One way to correct this problem is to halt traffic for 1-3 minutes so that a line-of-sight view with a tiepoint reflector can be established.

In regards to safety, provide the surveying team enough space to set up equipment at a safe distance from the roadway. Reflective vests or shirts should be worn at all times. To protect tiepoint reflectors and tripods, orange reflective cones are advised to be set up around these to make them more visible to motorists. It may also be prudent to weigh down reflector tripods so they do not fall over from vehicle turbulence. Finally, orange "ROAD WORK" or "SURVEY CREW" signs provide passing motorists an indication that the survey team is near.

Field Supplies

Prepare field supplies according to the environmental conditions of your scanning project. Be prepared to stand out in hot, humid, sunny days as well as windy, cold,

winter conditions. Proper attire and supplies such as sun screen, chapstick, sunglasses, field boots etc. should be considered.

Survey Team

An effective way to conduct a successful scanning survey is to build a team of a minimum of 4 people to maximize time efficiency. Commonly, two people can set up reflectors and the main LIDAR unit while the other pair sets up the RTK-GPS system and begins gathering GPS control points if needed.

2.) LiDAR Equipment

The following is an inventory of LiDAR equipment needed to conduct a scanning survey. Some of the equipment may not be necessary depending on the goal of the survey. For instance, if color photography is not needed then the camera is not required. Similarly, the RTK-GPS is not required if geoferencing of the LiDAR datasets is not a priority.

Lidar checklist

Laptop (Toughbook)

Honda Generator

Gas Can (1 gal.)

DC inverter

Battery (blue/gray)

Prism-Rod Holder-Laptop Tray Case
- -Laptop tray (w/ stand and 2 screws)
- -Screwdriver
- -Laptop shade
- -8 Rod holders
- -2 Levels
- -4 Prisms
- -8 Rod tips
- -GPS mount

Camera Case
- -Nikon D300 Camera on mount
- -3 Nikkor lenses (20mm, 85mm, 180mm)
- -Camera battery Charger
- -3 Camera batteries
- -Camera strap
- -USB cable
- -AC adapter and two-pronged outlet plug
- -Camera DVD
- -2 Allen wrenches

Reflectors-Targets Case
- -12 cylinder reflectors
- -3 Flat target canisters
- -White tape roll

Lidar Case
- -Scanner
- -Carrying handle
- -Allen Wrench
- -Fuses box
- -4 Green cables (90^0 angled cable, extension cable, 2 computer connect cables)
- -4 Gray power cables (90^0 angled cable, DC cable, red/black clamp cable, red/black banana end cable)
- -Tan computer cable
- -Tripod mount (in bubble wrap)

Tripod Case #1
- -4 Tripods
- -8 white/orange poles

Tripod Case #2

-4 Tripods
-10 white/orange poles

RTK-GPS checklist

Battery (black)

Solar panel (camo)

Range pole for Data Collector (with controller clamp)

Yellow Backpack

Golf Club Case #1
-Tripod
-2 Antennae Bags
-Unmarked Bag-
-Long Range Bag
-Extension pole
-Tripod disk
-Antenna clamp
-2 Antennae (long and short)

Golf Club Case #2
-2 Tripods

Large Yellow Case (STAR)
-2 GPS receivers
-Data collector
-Tape measure
-Tripod leveling plate
-3 receiver batteries
-Extension rod (0.25m)
-Short receiver antenna

Large Yellow Case
-AC inverter (light blue)
-Yellow power pack
-DC charger with AC plug-in
-AC battery chargers (2 chargers and 2 adapters)
-Data collector AC charger
-Large AC battery charger

Medium Yellow Case
-Positioning Data Link Box
-Dark gray power cable
-Black "Y" cable
-4 black pens
-2 Allen wrenches

3.) Georeferencing

Although georeferencing of LiDAR datasets is not necessary for some scanning projects, the following section describes the procedure for gathering GPS points and how these points are used to georeference LiDAR datasets. Currently, KU Geology has one type of GPS equipment available: A Trimble 5800 Real Time Kinematic (RTK)-GPS.

Trimble 5800 RTK-GPS

The Trimble 5800 RTK-GPS is a Real Time Kinematic (RTK) GPS collector capable of attaining GPS points with cm-scale accuracy. The advantage in using this set up to attain GPS control on the LiDAR data is that the collected GPS points are quickly gathered and then uploaded to the LiDAR software. Also, it is to the user's advantage to gather GPS points and georeference the LiDAR project prior to scanning. In other words, if an erroneous GPS point is collected and then imported into the LiDAR software, it is thrown out and re-surveyed prior to LiDAR scanning.

Hardware Setup

The following diagram illustrates the hardware setup of the RTK-GPS.

A. Base receiver

B. Power pack

C. Tribrach mount

D. Black "Y" cable

E. Gray cable

F. Positioning Data Link box

G. Long range antenna

H. Battery

I. Short mounting pole

1) Set up both tripods within a meter of each other > extend the legs of one of the tripods (this will be the tripod with the antenna mount)
2) On the shorter tripod > Screw on the Tribrach and level it > Screw on the 0.25 m yellow pole > Screw on the Base receiver > Measure the height to the bottom of the Base receiver (this height will be inputted into the controller setup)
3) Insert the single end of the Black "Y" cable into the Base receiver
4) Hang the Power pack on the short tripod and connect its cable to one of the ends of the Black "Y" cable
5) Screw the Long range antenna onto its mounting pole and extend the pole > Screw the pole and antenna onto the tall tripod
6) Hang the Positioning Data Link box onto the tall tripod > Screw on the cable from the Long range antenna into it > Plug in the Gray cable
7) Connect the last end of the Black "Y" cable into the Gray cable > Connect the Gray cable to the Battery
8) Turn on the Base receiver

A. TSC2 controller

B. Rover receiver

C. Rover antenna

D. Range pole

1) Attach the TSC2 controller onto the Range pole and controller holder

2) Screw the Rover receiver onto the Range pole

3) Adjust the height of the range pole to a comfortable setting (this height will be recorded in the controller setup)

4) Attach the Rover antenna clamp to the Range pole > Screw the Rover antenna onto the clamp > Screw the Rover antenna cable onto the Rover receiver

5) Power on the Rover receiver

Controller Setup

The following are instructions for initialization and setup of the TSC 2 handheld controller.

Powering On:

1) Power up base receiver and radio by pushing the Power button on each of the receivers
2) Power up the controller by pushing the green power button in the lower left corner of the controller
    a. Hold the power button down for 5 seconds to reboot the controller
3) Start "Survey Controller" Software from the start menu or push the survey controller software button

Creating a new job:

1) Files > New Job
    a. Enter Job Name
    b. Select coordinate system – (e.g., UTM zone 44 N)
    c. Leave remaining fields as default
2) Press "Enter"

Starting a survey:

Starting a survey is a two step process. First the base receiver must be set up and initialized. Second, the rover must be initialized.

Base receiver setup/initialization:

1) Configuration > Controller > Bluetooth
    a. Select ***493 receiver

2) Press “Accept”

! Note: Controller must be in ‘line-of-sight’ with the receiver z!

3) Survey > RTK > Start Base Receiver

   a. “Connecting to Receiver” dialog appears

   b. Select a base point (“List”) or key in a new one (“Key In”)

   c. If entering a new point, use the “HERE” button to fill in location

4) Press “Store”

5) Measure and Enter “Antenna Height” with the appropriate units

6) Press “Start” / “Enter”

7) Press “OK” when “Disconnect controller..” dialogue appears

8) Confirm connection by icons on upper right of screen

Rover Initialization / Survey Start:

1) Configuration > Controller > Bluetooth

   a. Select ***601 receiver

2) Press “Accept”

3) From the Main Menu, Survey > RTK > Start Survey

   a. Start survey menu pops up

   b. When reliability reaches 100%, hit “Accept”

4) Confirm survey start by checking for H and V data at the bottom of the screen

Collecting data points:

1) From the Main Menu : Survey > Measure Points

2) Set Point name and code (point names automatically roll over)

3) You may set precision limits through the “Options” button

Changing Frequency:

1) Configuration > Survey Style > RTK > Rover Radio
2) Press Connect
3) Connecting to radio dialogue appears
4) Arrow by frequency, select channel
5) Hit accept
6) Connecting to radio dialogue appears
7) Press store

Exporting Data:

1) Connect the controller to the Toughbook via USB cable
2) Active Sync should appear
3) On the controller, Go to Files > Export fixed file formats
4) Check to make sure that all of the fields are accounted for in the next screen
5) Press Enter > All Points
6) In Active Sync, go to Explore > Windows Based Mobile Devie > Trimble Data
7) Locate the exported file in this folder and copy and paste it to a folder on the Toughbook hard drive

4.) Tiepoint reflector setup

Tiepoint reflectors are a way to merge data gathered from different locations (also called scan positions) within a study area. By identifying these reflectors within the LiDAR data, RiScan Pro can merge each data set with cm-scale accuracy while attaining complete data coverage of an area. For referencing and merging accuracy, place at least four tiepoint reflectors around the study area in a non-linear arrangement. Be sure to set the tiepoint reflectors in locations where the LiDAR scanner will be able to see each of them no matter where the scanner is placed (See Figure 20 in Methods section).

The following are an inventory and diagram on how to setup a tiepoint reflector.

Tiepoint reflector setup:

A. Cylindrical reflector or prism

!Note: Do not operate LiDAR scanner within 100m of a prism!

B. Tripod

C. One or two 4 ft. range poles

Use 4 ft. pole during high winds and 8 ft. pole for better visibility

D. Black plastic pole clamp

E. Metal pole tip

- Fish-eye pole level for setup (not pictured)

1) Attach the black pole clamp onto the tripod by screwing the tripod bolt into the clamp
2) Screw on metal tip to the end of the pole(s)
3) Insert the other end of the pole into the cylindrical reflector or screw on a tiepoint prism
4) Place the tip of the pole onto the point of reference (presumably the point of reference has already been surveyed) and place pole in black plastic clamp
5) Adjust and set tripod so that the pole is plumb

5.) LiDAR scanner setup

The Riegl LMS-Z620 LiDAR scanner weighs ~60 lbs. and therefore requires great care while transporting and lifting it. The scanner sits atop a tripod which should be situated on a surface that insures the tripod legs will not be disturbed or moved during operation. As a reminder, be sure the area where the scanner is set up in a location that has line of sight to a minimum of 4 tiepoint reflectors. The following is a list of equipment and steps required for proper set up of the scanner.

LiDAR scanner set up equipment list:

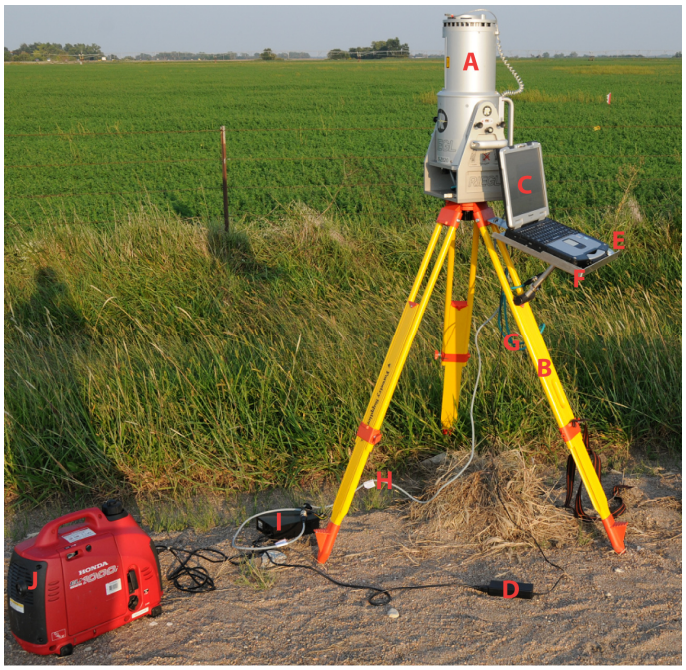

A. Riegl LMS-Z620 LiDAR scanner

B. Tripod (*with screw-locking legs- do not use quick-locking tripods)*

C. Panasonic Toughbook

D. Toughbook Charger

E. Computer mouse

F. Laptop Tray

G. Two-piece teal Ethernet scanner-to-computer cable

H. LiDAR scanner power cable with banana plug connecting piece

I. AC to DC converter with female banana outputs

J. Honda generator

- Fish-eye tripod level (not pictured)

- Nikon D300 digital camera with battery (not pictured),*only necessary if point color data is required*

LiDAR scanner set up instructions:

Tripod set up:

1) Set up the tripod first on a ground surface that is stable and use the fish-eye level on the top flat plate of tripod (be sure that the tripod legs are tightened)
2) Open the LiDAR case and attach the lifting handle to the back of the scanner
3) With two people, lift the scanner out of the case and gently set it atop the tripod
4) Screw in the tripod mounting bolt and point the back of the scanner toward an area that is of lesser importance (the scanner produces a small gap in the data toward the area directly at the back side of the scanner)

Tilting Scanner:

1) To attach the camera, power cable, and Ethernet cable, pull out the six black knobs on the side of the scanner in order to tilt the scanner downward
2) Slowly rotate the scanner downward until the cable ports are accessible and the camera can be safely mounted, Set one of the six black knobs on the side of the scanner to lock it in place

3) Make sure that a fresh battery is in the camera, the proper lens is mounted on the camera, it is turned on, and that the mini-USB cable from the scanner is plugged into the bottom of the camera
4) Mount the camera on top of the scanner by inserting the black rectangle set into the proper hole on top of the scanner and turn the camera mount into place
5) Screw in the bolt on the camera mount to properly put the camera in place
6) Screw in the elbow end of the gray power cable into the bottom of the scanner
7) Screw in the elbow end of the green Ethernet cable into the bottom of the scanner
8) Unlock the black peg on the side of the scanner and slowly rotate the scanner back to vertical and lock in the 6 black pegs

Power system:

1) Set the Honda generator close to the tripod and make sure that it is full of gas
2) The breather switch on the gas cap and the kill switch on the side of the generator should be set to "ON"
3) Switch the choke to "ON" and fully pull the starter cord until the generator powers up
4) Wait a few seconds for it to warm up and turn the choke to "OFF"
5) Plug in the Laptop charger and the DC converter into the generator
6) Plug the red/black banana end plugs on the gray power cable into the converter
7) To power on the scanner screw the end of the banana plug cable into the power cable from the scanner
8) Turn the kill switch to "OFF" to shut off the generator

Laptop setup:

1) Screw the laptop tray together and hook it onto one of the tripod legs that is most convenient
2) Plug the green Ethernet cord into the Ethernet port and plug the charger into the laptop
3) Power up the laptop and plug in the camera cord and the mouse into two USB ports

6.) LiDAR Acquisition

This section details how to properly run the LiDAR software (RiScan Pro 1.4.3) to acquire point cloud data. Knowing the level of resolution needed, how long each high resolution scan will take, and budgeting enough time to acquire enough data are important aspects in gathering LiDAR data. Merging each successive scan position together in the field is also recommended so that additional data can be gathered if necessary. The following step-by-step instructions are all within the RiScan Pro software.

RiScan Pro

Setting up the project:

1) Open RiScan Pro
2) Click Project > New
    a. Name the project > Click OK
3) Under Project Manager > Expand Calibrations Folder
4) Camera
    a. Right Click Camera > New Camera Calibration (blank)…
    b. Click Import… > From project…
    c. Open the appropriate Default Project (20mm, 85mm, 180mm) for the lens that is attached to the camera > Double click on the project.rsp
    d. Click the Result calibration final > Click OK
    e. In the New Camera Calibration dialog box, Click OK
5) Mounting
    a. Right Click Mounting > New Mounting Calibration (blank)…

b. Click Import… > From project…

c. Click on the project.rsp file within the Default Project xxmm folder that was loaded during the Camera Calibration > Click OK

d. Click the Result calibration final > Click OK

e. In the New Mounting Calibration dialog box, Click OK

6) Reflector

a. Expand the Reflector folder

b. Add the cylindrical reflectors by Right Clicking on the Reflector folder > New Reflector…

c. Name the new cylindrical reflector (i.e. Riegl cylinder 10 cm)

d. Change Reflector Shape to Cylinder

e. Input the proper measurements (0.10 m Diameter, 0.10 m Height for Riegl cylindrical reflector)

7) Scanner Orientation

a. Check the level of the scanner by going to Tool > Scanner orientation

i. The dialog box shows the current orientation/level of the scanner (ideally this should be within 3 degrees)

Importing GPS coordinates

1) In the Project Manager, open TPL (GLCS) which stands for TiePoint List (Global Coordinate System)

2) Click Import tiepointlist… > Navigate to the file that has the GPS control points > Click OK

3) An Import tiepointlist… dialog box pops up where the individual points in the file are listed and can be assigned the proper designation
    a. Make sure that the points are separated with the correct delimiter (comma, tab, space, etc.)
    b. Drag the appropriate column header from the Column Association section into the proper header within the PREVIEW section (Name, X, Y, Z) > Click OK
4) Within the TPL (GLCS) window, highlight all of the points > Right Click > Copy tiepoints to… > TPL (PRCS) which stands for TiePoint List (PRoject's Coordinate System) > Use original name > Type in 0, 0, 0 for the Translation to POP Matrix coordinates (No translation is needed for the GPS points)
5) Close the TPL (GLCS) window

Scanning

1) Within the Project Manager > Right Click on Scans > New Scanposition > Keep default name > Click OK
2) Expand ScanPos001 > Right Click on ScanPos001 > New single scan
3) The New single scan dialog box pops up
    a. If the object/area of interest and the tiepoints are within ~100m, Click Overview (which has a resolution of 0.201 mrad) > Check the Image Acquisition box if images are to be needed > Click OK > Click OK to start scan
    b. If the object/area of interest and the tiepoints are >100m, Click Panorama (resolution = 0.120mrad, or adjust up to 0.800mrad) > Click the equal

button to calculate a new scan completion time > Check the Image Acquisition box if images are to be needed > Click OK > Click OK to start scan

4) 2D view
    a. When the initial 360° scan is complete, a 2D view of the scanned data opens in RiScan Pro
    b. Identify each tiepoint reflector in the 2D view
    c. Zoom into the tiepoint and Left Click > without moving the mouse, Right Click > Add point to TPL > categorize the tiepoint as either a cylinder or prism > Click OK
5) Fine Scanning Tiepoints
    a. In the ScanPos00x folder, Open TPL (SOCS) TiePoint List (Scanner's Own Coordinate System) > Highlight all of the tiepoints that were picked out from the previous step > Click Finescan selected tiepoints 
    b. The scanner will go through each tiepoint and find the exact center of that reflector to more accurately reference the dataset
        i. Examples of good tiepoint finescans:

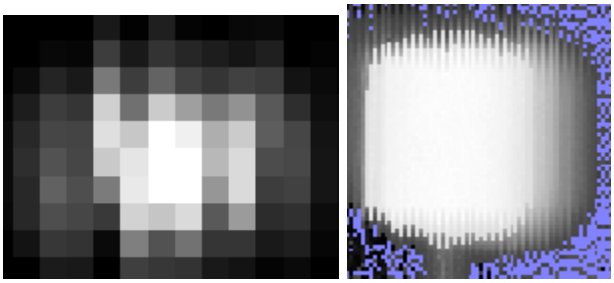

        ii. Under the Size column in TPL (SOCS), cylinder reflectors should have a size of ~0.10m and prisms should have a size of ~0.30m

c. To rescan a bad tiepoint, highlight that tiepoint and Click Finescan selected tiepoint

6) Fine Scanning

a. In the Project Manager, Right Click on the 360° scan > New single scan

b. In the New single scan dialog box, Hold the Alt key while dragging a box with the left mouse button to subset an area within the 2D view from the previous scan

c. Adjust the scan resolution to achieve the desired level of resolution > Click the equal button to calculate a new scan completion time

d. Click OK > Click OK to start the new fine scan

Setting Reflector Heights

e. Each pole-mounted reflector or prism represents a point on the ground, therefore the height above ground of each needs to be inputted

f. In the Project Manager, Open TPL (PRCS) TiePoint List (PRoject Coordinate System)

g. For each tiepoint, Right Click > Set reflector height > Input reflector height in meters (For single poles = 1.219m, double poles = 2.438m)

i. Be sure to repeat this step as the TPL (PRCS) list becomes populated with more tiepoints

Georeferencing/Merging

h. In the ScanPos00x folder, Open TPL (SOCS) > Click Find corresponding points… 

i. In the Corresponding points dialog box, Check the box next to Project Coordinate System
    i. As more scan positions are added to the project, referencing datasets to each other will be possible by checking the appropriate boxes beside the added scan positions
j. Set the Tolerance value initially at 0.100m > Click Start
    i. RiScan Pro will attempt to find a match between the GPS coordinates that were imported and the tiepoints that were fine scanned
    ii. It will display a number of how many GPS points were matched up within the Tolerance value and their standard deviation
    iii. Open the TPL (SOCS) list for each Scan position in the background and it will show which reflectors are matching up with the control points
k. Click Next to calculate a different combination of tiepoint links
    i. Usually the first solution is the best
l. If no points are found, increase the Tolerance value
m. Click OK to accept the current tiepoint links

Additional Scan Positions

1) When gathering additional data and setting up the scanner in other locations around the project site, repeat all of the steps starting with the **Scanning** section
2) Be sure to merge each dataset as described in the **Georeferencing/Merging** section before the scanner set up is disassembled

3) Preview data from each scan position by going to the Project Manager > Double Click the single scan > A dialog box appears that gives different options for displaying the data > Select 3D > Click OK

Camera Referencing

1) Within each scan position there is a list of photos taken by the camera and a list of the scans that were gathered
2) Open 2 or 3 photos that have tiepoint reflectors within the picture by expanding the ScanPosImages list within a scan position > Double Click the photo to open it
3) Display the location of the tiepoint reflectors by pushing Ctrl+2, the location of the tiepoint will not match the tiepoint reflector imaged in the photo
4) Zoom in to each tiepoint reflector in each image and Left Click on the center of the tiepoint > Right Click > Add point to TPL > Zoom out so that the entire photo is visible
5) Right Click within each photo > Auto Linker > Change pixel number to at least 100 > Click OK
6) In the Project Manager, Double Click the Mounting calibration that the photos were taken with
7) Click on the Re-adjustment of camera mounting tab > Start re-adjustment
8) In the Log/Best Results section, the Pixel distance mean should be around 2-5 > Click OK
9) If the pixel distance is larger than this, delete the tiepoint links within the photo's TPL list (under the ScanPosImages list and within each photo) and redo steps 2-8

10) Repeat this process for each scan position and the photos taken from each scan position

Coloring Point Cloud Data

1) Color a scan with RGB values from the photos by Right Clicking a scan > Color from images > Select the appropriate photos > Click OK
2) A new "ColorScanPosXX" appears

Exporting Point Cloud Data

1) To export each scan, Right Click on the specific scan > Export…
2) Navigate to the folder where the scan data is to be stored > Click OK
3) In the Export pointcloud dialog box, select Project coordinate system (PRCS)
4) Make sure that the boxes are checked next to X, Y, Z, RGB (if photo pixel data from the camera was gathered), and Amplitude
5) Set the Separator as comma > Click OK
    i. The data is now exported as an ASCII file that is a comma delimited list of each point

7.) Post-Processing

Post-processing of the raw LiDAR acquired from the field is done within Bentley's Microstation, which is an CAD software. The software application that filters and classifies the data is TerraScan, which is developed by TerraSolid Inc. TerraScan is an application that is loaded and utilized within Microstation. TerraSolid also produces another application, TerraModeler, which creates surface models of the LiDAR point clouds. It is worth noting that TerraScan and TerraModeler were developed for use with airborne LiDAR data. However, they are still effective at manipulating TLS data. The following sections are brief descriptions of TerraScan and TerraModeler with subsequent instructions for using Microstation, TerraScan, and TerraModeler.

TerraScan

The main goal in using TerraScan is to classify the raw LiDAR data imported from RiScan Pro. TerraScan uses a set of algorithms with tolerances that are set by the user to come up with a classified point cloud. This classified point cloud is separated into ground points, vegetation points and erroneous low points. Once this task is completed, exporting the ground points, which represent a bare-Earth surface, is possible.

TerraModeler

TerraModeler is a supplementary program that creates contoured surfaces, hillshaded surfaces, and other methods for displaying the point cloud data. The surface that is created within TerraModeler is a Triangular Interpolated Network (TIN) surface. It will only create a TIN surface in XY space. It will not effectively create a TIN surface of a subvertically oriented point cloud (i.e. a vertical rock outcrop).

Microstation Design File

1) Open Bentley's Microstation software
2) A design file (.dgn) will need to be created first, in Microstation Manager > File > New > Name the new .dgn file (be sure that the seed file has "seed3d.dgn" selected, if not Click select and Click on seed3d.dgn) > Click OK
3) In Microstation Manager, Click OK
4) In Microstation, Click Utilities > MDL Applications
5) Scroll down and Click on TSCAN > Click Load
6) Click on TMODEL > Click Load > Close MDL Applications dialog box
7) Close out Views 3 & 4 to create an open working space
8) Go to Window > Tile to arrange Views 1 & 2 side by side

Microstation Tools

1) In Microstation's main toolbar there are three main tools which are utilized:
    a. Fence tool  - Creates a fence around LiDAR points by dragging a box or creating multiple lines to make a polygon (polygon can be closed by snapping the last segment to the initial starting point of the polygon)
    b. Smartline tool  - A Smartline is used to make successive 2D profile slices which will be explained later (Left Click to start a Smartline and Right Click to end a Smartline)
    c. Selection tool  - Selects only Microstation elements such as Smartlines

d. Accudraw  - Provides X, Y, Z coordinates of the point where the cursor is hovering (To get true readings of coordinates, retrieve XY coordinates from data that is in true mapview- retrieve Z coordinate from a cross section view)

e. Rotate Image  - In each view window, rotate the view by scrolling in or out and using the rotate view tool at the bottom of each view window by Left Clicking once to activate and a second time to set view

f. Measure a Distance  - Click once to start a line and Click twice to measure the distance of that line

TerraScan Tools

1) The following are commonly used tools in TerraScan

a. Cross Section  - Click once to start a cross section line in View 1 > Click again to end the cross section line > Adjust the thickness of the cross section by moving the mouse > Click a third time to display the cross section in another View window

b. Travel Path  - Place a Smartline along a path perpendicular to how the cross sections will be viewed > Click on the Smartline to activate it > Click the Travel Path tool > Set the parameters in the Travel Path

window: 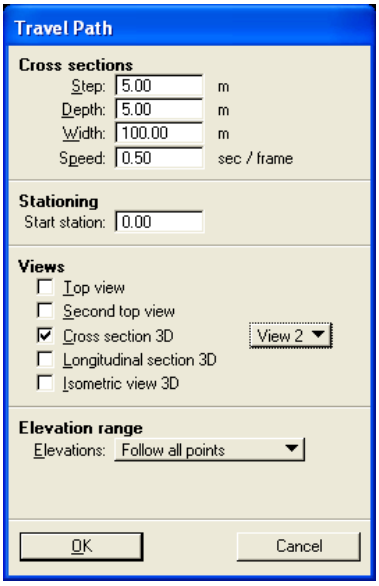

> Click OK > Control Travel Path cross sections with the Travel Path toolbar:

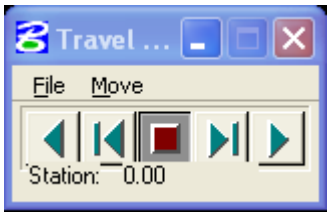

c. Classify below line  - Click once to start a line > Click twice to classify all points below the line from one class to another by using the Classify below line toolbar: 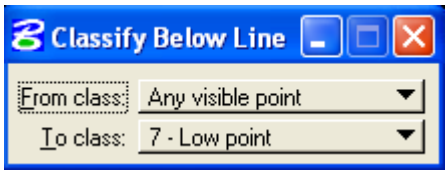

TerraScan- Reading Points

1) Once TerraScan is loaded, a side toolbar appears as well as the main toolbar:

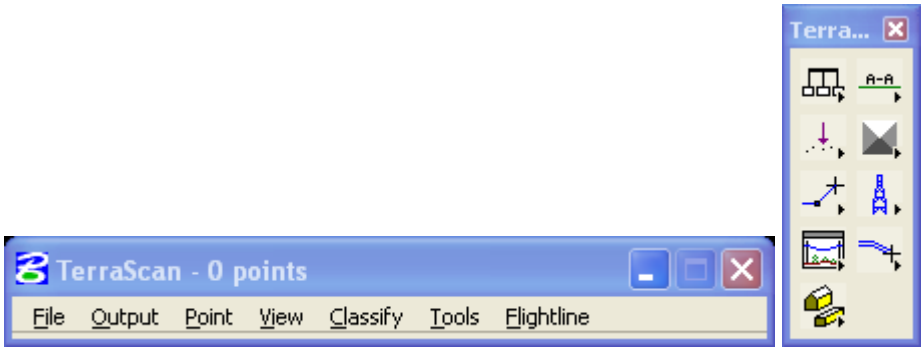

2) To read in LiDAR points from RiScan Pro, Click Settings-  > In the TerraScan settings dialog box, Click File Formats > User point formats > Click Add
3) In the File format dialog box, Click File > Load example… > Navigate to one of the exported RiScan Pro files > Click OK
4) Assign the proper column headings to the file format by first Clicking on No field > Name the file format in under Format name > Click OK
5) Close out of the TerraScan settings dialog box
6) In the main TerraScan toolbar, Click File > Read points… > Navigate to the exported RiScan Pro files > Select all of the files > Click Add > Click Done
7) In Load Points dialog box, make sure that the proper file format is selected and that the Load color values box is checked if necessary > Click OK

TerraScan- Classifying Low Points

1) Classify the erroneous Low Points by using the marching cross section marching tool and the Classify below line tool
2) Place a Smartline across an area where Low Points are probable > Select the Smartline by using the Selection tool and Click on it

3) Click on the Travel Path tool > Set the Step (how far along the Smartline it will move at a time)
4) Set the Depth (how thick the cross section will be)
5) Click on the box to Apply the view to view 2 > Click OK
6) A Travel Path dialog box with appear with controls to travel along the Smartline
7) Go through each cross sectional slice and use the Classify below line tool to Classify the Low Points

TerraScan- Macro Routines

1) Once all of the Low Points are classified run a Macro on the points by going to the TerraScan menu > Tools > Macro
2) Open a Macro that is already made:

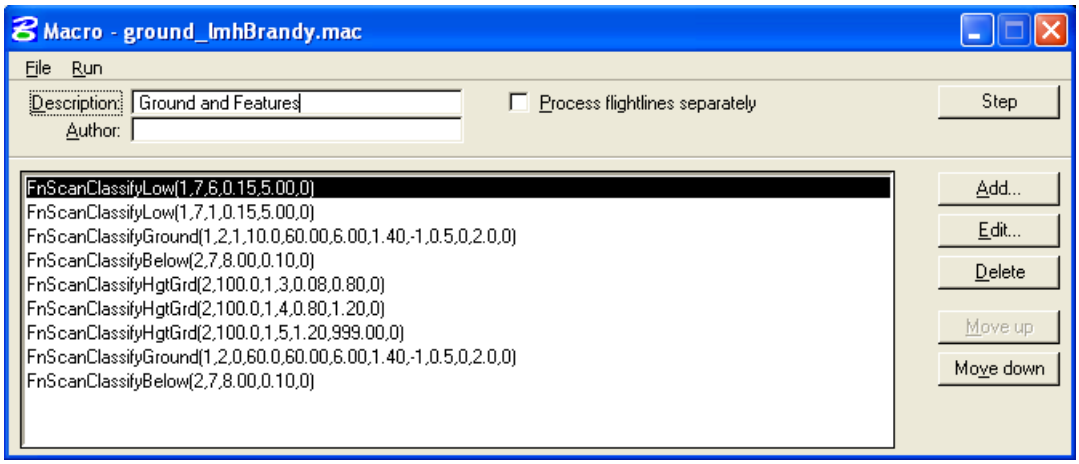

3) Macro Routines:
    a. Classify Low- Classifies an individual point or a group of points that are anomalously below the points in the surrounding area

b. Classify Ground- Classifies Ground Points based on an adaptive TIN model where the Ground Points are populated upward from initial seed points and search parameters that define certain geometric criteria.

c. Classify Below- Classifies Low Points from the Ground class in a manner similar to Low Point classification

d. Classify Height Above Ground- Classifies Default Points that were not classified as Ground into ranges of Vegetation Points above the Ground Points

4) Adjust the tolerances for the Ground routine and Low Point routine accordingly for the type of terrain that was scanned

a. Most importantly, the Ground routine is based on three parameters:

Terrain Angle- This should be set at an angle that is approximate to the slop of the terrain. However, set the Terrain Angle to 88°-89° if there are vertical objects in the scan area

Iteration Angle- The iteration angle is a search tolerance that is an angle above the edge of a horizontal TIN triangle where any point that lies within this angle is classified as Ground

Iteration Distance- The iteration distance is another search tolerance that defines how far away from a Ground seed point the search window will reach. (For more discussion on these parameters refer to the Methods section of Chapter 2)

5) Click Run > On loaded points

6) Check to see if the Macro did a sufficient job of classifying the points, if not, rerun the Macro with adjusted parameters
7) To export the Ground point class go to the TerraScan main toolbar > File > Save points as... > A dialog box will appear that provides different ways to save to points > Click on Ground > Make sure that the proper file format is selected > Click OK > A save dialog box appears > Name the points and type ".txt" behind the file name > Click Save
8) The exported points will be organized by columns and tab/space delimited

ArcMap DEMs

ArcMap has a variety of ways to create a raster file of LiDAR points. The heterogeneity of TLS data proves to be the most challenging aspect when making a surface of the points. However, the Radial Basis Function in ArcMap is usually the most effective way of making a surface model from TLS data. Unlike the Kriging or Inverse Distance Weighted interpolation techniques, the Radial Basis Function does not create sharp edge artifacts that are sometimes produced in the two former methods. This section describes how to create a surface model from LiDAR Ground points exported from TerraScan.

ArcMap

1) Before the data is brought into ArcMap, be sure to format the exported Ground point cloud correctly by having it as a comma delimited text file with a header at the top that is labeled as "X,Y,Z"
2) Once the data is in the proper format, Open a new blank map in ArcMap
3) Go to Tools > Add XY Data...

4) An Add XY Data dialog box appears > Select the Ground point text file > The header fields X & Y should appear in the X Field & Y Field drop down boxes
5) Click Edit... > Select... > Projected Coordinate Systems > UTM > Select the proper datum (e.g. NAD1983, WGS 1984, etc.) > Navigate to the proper UTM zone (e.g. 14N) > Click Add > Click OK > Click OK
6) A new Events layer appears in the Table of Contents, Right Click on this layer > Data > Export... > A new dialog box appears, name the new shape file and select its destination > Click OK > Click Add this new layer to the current map
7) In the Geostatistical Analyst extension, open the Geostatistical Wizard
8) Click on Radial Basis Functions > Select the newly created shape file as the Input data > Select the Attribute as Z > Click Next
9) In the next step in the Wizard, in Kernel functions > Select Spline with Tension > Leave the rest as default > Click Next
10) The final step in the Wizard displayed the average RMS errors for the interpolation, this is the RMS of the point cloud from the Radial Basis Function surface, Click Save cross validation to save the error values for each point
11) Click Finish > Click OK
12) A Radial Basis Functions Predictions Map appears in the Table of Contents
13) Export this new layer as a raster file, Right Click on the new layer > Data > Export to Raster > Select a name and destination for the file> Input a raster cell size > Click OK

14) The new raster file is the interpolated surface model for the LiDAR Ground points

MATLAB Plots

Since making XY profile plots in Microsoft Excel is somewhat tedious, MATLAB provides an efficient way to plot the thousands of data points that exist in any profile line. However, some file calculation is needed in Excel before these profile can be made. This section details how to create swath profile of LiDAR in MATLAB. This assumes that you have already fenced off a profile of interest in TerraScan and have saved that profile as a comma delimited (.csv) file which will be read into MATLAB.

1) Since the profile is likely taken as a diagonal line relative to the coordinate system that the data are in, a root-squared manipulation must first be done, Open the profile data in Excel > In a blank column calculate the straight line distance along the profile points by using the following equation:

```
=sqrt((ColumnA^2)+(ColumnB^2))
```

2) Save the new coordinate and its corresponding Z value as a new .csv file with the straight line coordinate in Column A and the Z value in Column B
3) Open MATLAB > In the Current Directory > Navigate to the folder where the profile data is stored
4) The profile that will be plotted should be displayed in the Current Directory sub-window
5) First the comma delimited data will be read into MATLAB, give the .csv file (in this example ProfileA.csv) a variable name for use in MATLAB such as ProfileA and follow the following script as an example:

```
>>ProfileA = csvread('ProfileA.csv')
```

6) Assign a variable designation to the X coordinate by using the following script:

```
>>X = ProfileA(:,1)
```

6) Assign a variable designation to the Y coordinate by using the following script:

```
>>Y = ProfileA(:,2)
```

7) Plot the X and Y values using the following script:

```
>>plot(X,Y)
```

8) MATLAB's Figure dialog box appears that has the plotted data

9) Use the editing tools within the Figure window to change the display of the plot